

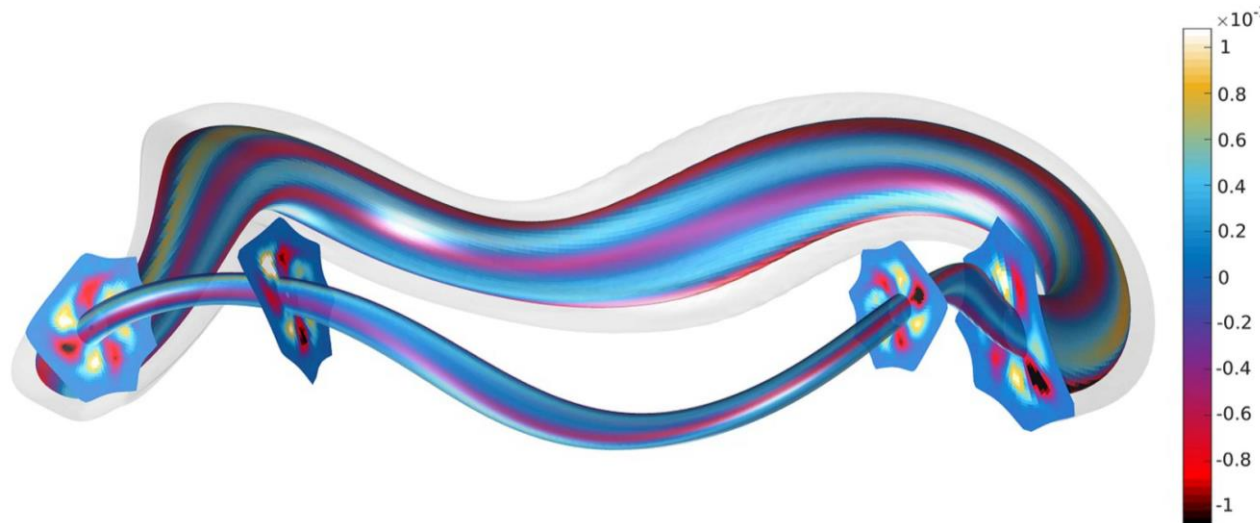
Kinetic-MHD hybrid simulations of energetic-particle driven instabilities

Yasushi Todo (National Institute for Fusion Science, Japan)



12th ITER International School

“The Impact and Consequences of Energetic Particles on Fusion Plasmas”
(26-30 June 2023, Aix-Marseille University, Aix-en-Provence)



[P. Adulsiriswad+, NF 60, 096005 (2020)]

Outline

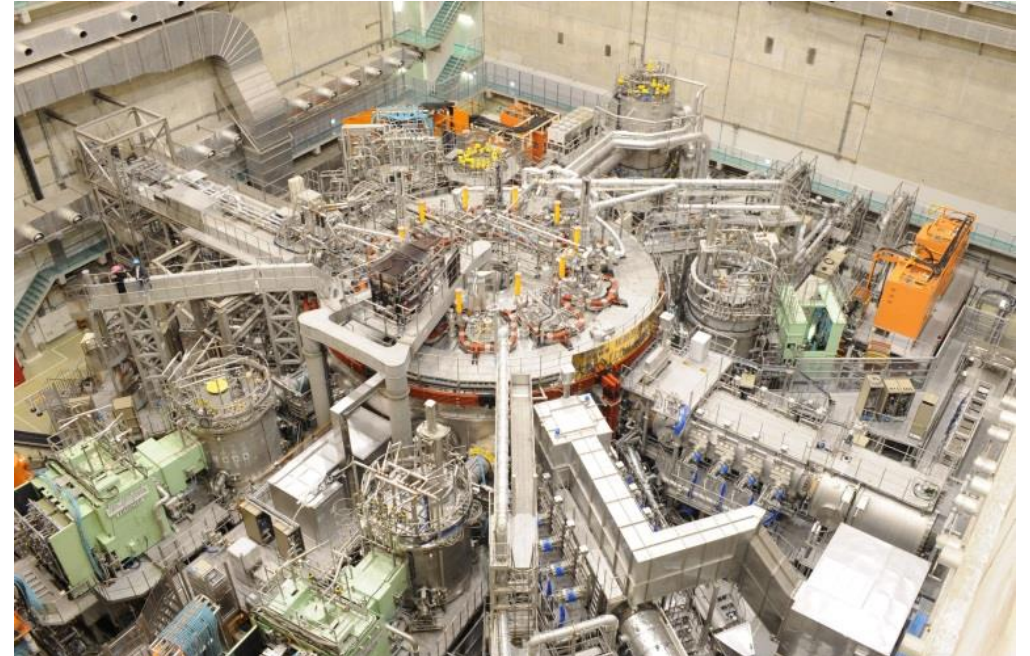
- Energetic particles (EPs) and Alfvén eigenmodes (AEs) in fusion plasmas
- Resonance condition, conserved quantity, and inverse Landau damping
- Phase space islands created by particle trapping and higher-order islands
- Nonlinear evolution of a bump-on-tail instability and frequency chirping
- Kinetic-MHD hybrid simulation
- Hybrid simulation for EP and MHD
 - Nonlinear MHD effects and zonal flow generation
 - Validation on DIII-D experiments (fast ion profile flattening and stiffness, electron temperature fluctuations)
 - AE burst and critical fast-ion distribution (profile resiliency)

Energetic particle confinement is important for fusion energy

- Nuclear fusion: safe and environmentally friendly energy source in the next generation
- Fusion reaction of deuterium (D) and tritium (T) in high temperature plasmas
$$D + T \rightarrow {}^4\text{He} \text{ (helium, 3.5 MeV)} + n \text{ (neutron, 14 MeV)}$$
- Energetic He (alpha) heats the plasma
- Confinement of energetic alpha particles are important for the sustainment of high temperature ($>10\text{keV}$)

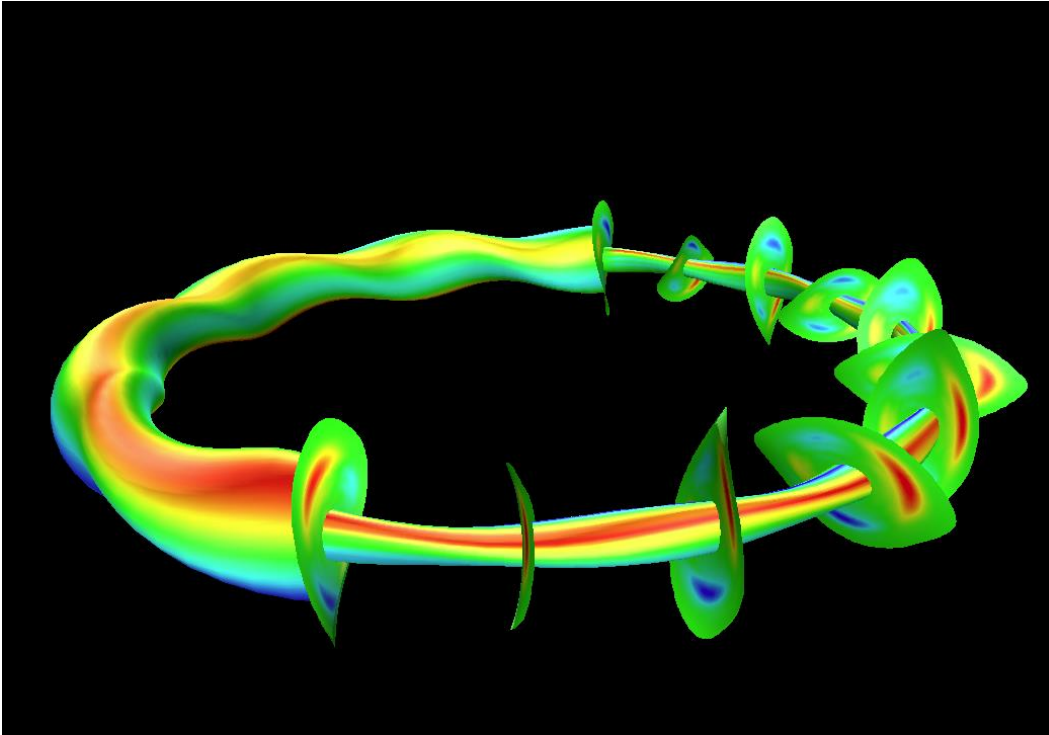
Energetic particles in fusion plasmas

- Alpha particle born from D-T reaction
 $D+T \rightarrow He^4 (3.5\text{MeV}) + n (14\text{MeV})$
- Neutral beam injection (NBI)
- Ion cyclotron heating (ICH)
- Electron cyclotron heating (ECH)

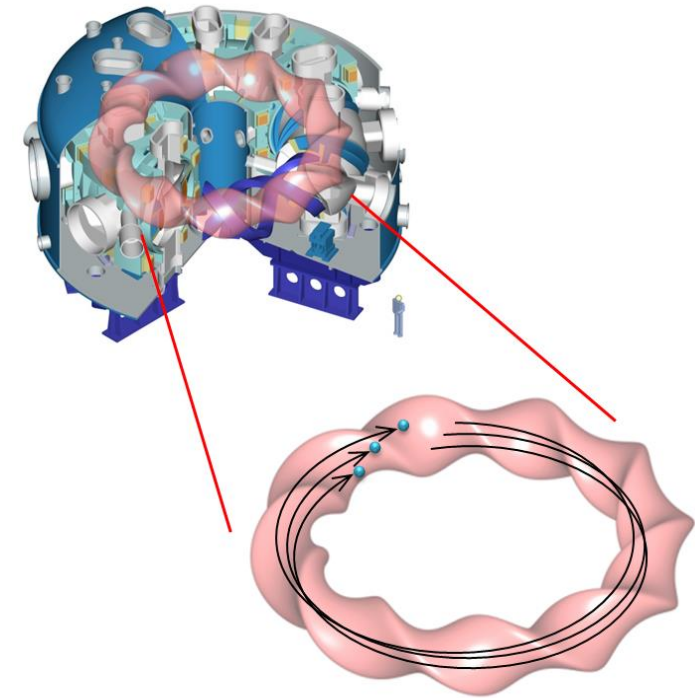


Large Helical Device (LHD)

Interaction between Alfvén eigenmodes (AEs) and energetic particles

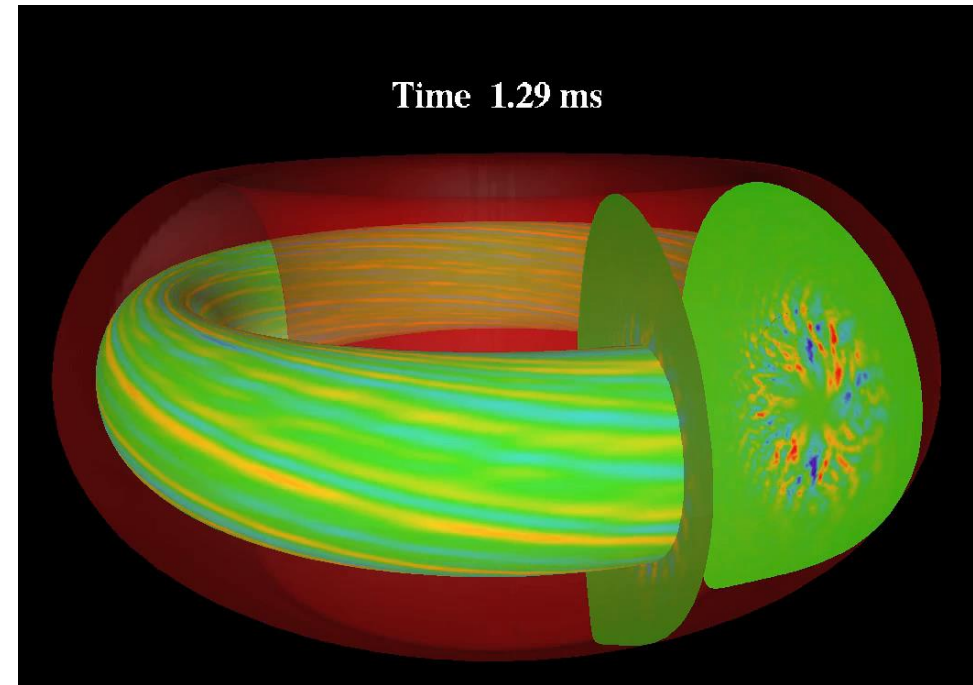
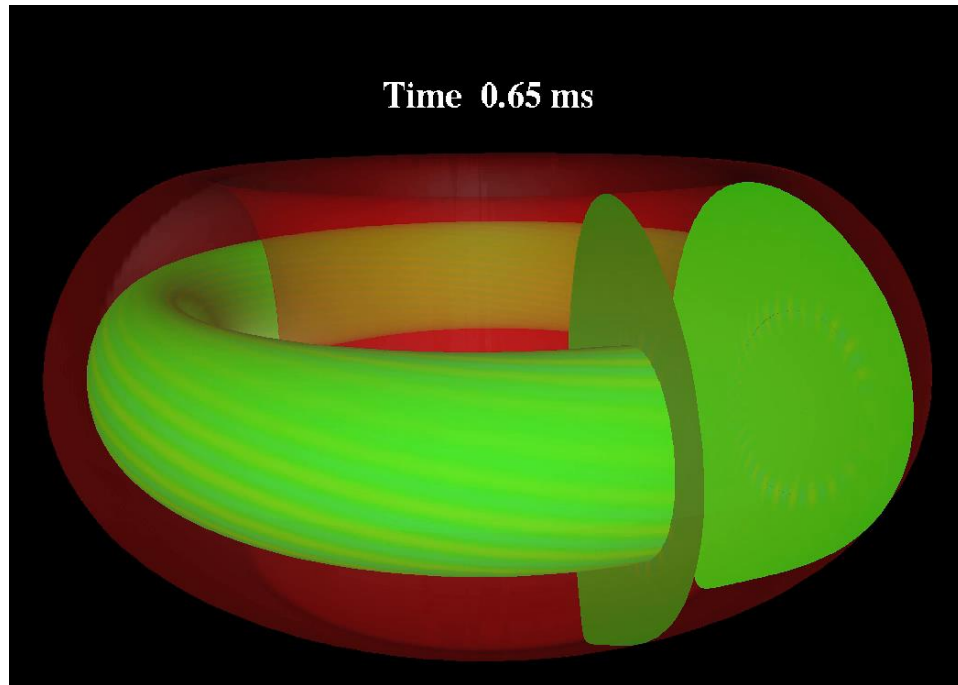


Alfvén eigenmode (magnetohydrodynamic oscillations) in LHD.



Energetic particles circulating inside the plasma interact with and destabilize AEs.

Time evolution of Alfvén eigenmodes in an ITER steady state scenario



Y. Todo and A. Bierwage,
Plasma and Fusion Research **9**, 3403068 (2014)

Is the interaction between EP and AE an important research subject in (plasma) physics?

- This is a problem of inverse Landau damping
 - with MHD waves
 - in 3D magnetically confined plasma (complicated particle orbit)
 - with non-uniform spatial distribution (spatial distribution is important as well as velocity distribution)
 - extended with source and sink (open system, EP distribution formation process, steady and intermittent evolution)

INTERACTION BETWEEN EP AND AE

Resonance condition in toroidal plasmas (1)

- When a resonant particle passes one round in the poloidal angle, the phase of the AE should change by a multiple of 2π .

This gives the resonance condition:

$$\omega * T_{\theta} - n * \Delta\varphi = L * 2\pi$$

T_{θ} : time for the particle to pass one round in the poloidal angle

$\Delta\varphi$: toroidal angle which the particle passes in T_{θ}

L : integer

- $\omega - n * \omega_{\varphi} - L * \omega_{\theta} = 0$

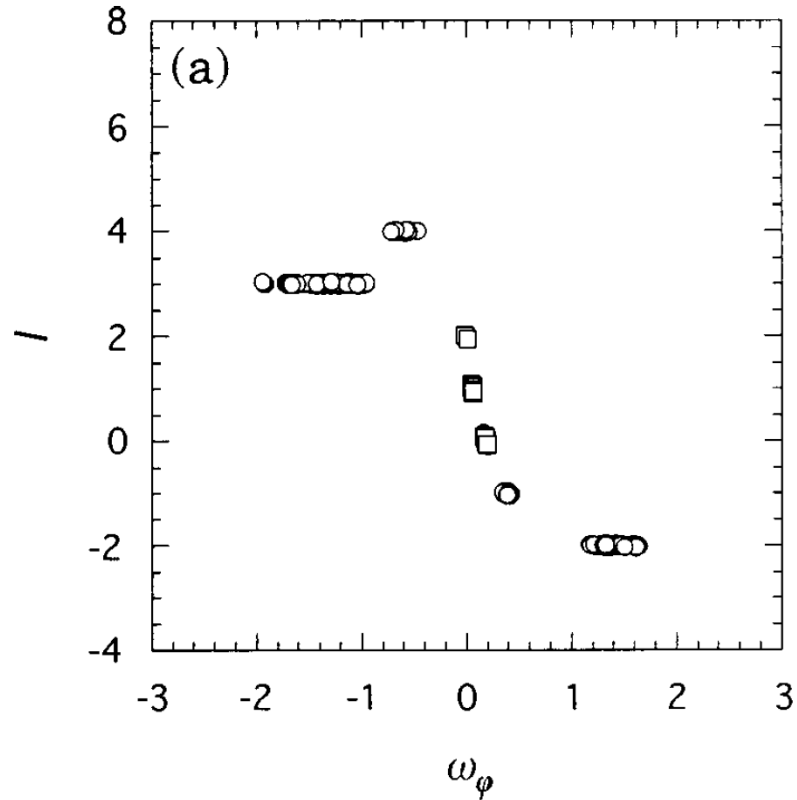
$$\omega_{\varphi} = \Delta\varphi / T_{\theta}$$

$$\omega_{\theta} = 2\pi / T_{\theta}$$

$$\text{or } L = (\omega - n * \omega_{\varphi}) / \omega_{\theta}$$

Resonance = When a particle passes one round in the poloidal angle, the phase of the wave is the same as that at the previous visit.

Resonance condition in toroidal plasmas (2)



Particles strongly interacting with an Alfvén eigemode in the simulation.

Integer => Resonance

Large delta-f particles interacting with a TAE

Vertical axis: $(\omega - n * \omega_\phi) / \omega_\theta$

Horizontal axis: ω_ϕ

[Todo and Sato, Phys. Plasmas **5**, 1321 (1998)]

Higher-order resonance

- When a resonant particle passes K rounds in the poloidal angle, the phase of the AE should change by a multiple of 2π .

This gives the higher-order resonance condition:

$$K * (\omega * T_\theta - n * \Delta\varphi) = L * 2\pi$$

T_θ : time for the particle to pass one round in the poloidal angle

$\Delta\varphi$: toroidal angle which the particle passes in T_θ

L : integer

- $\omega - n * \omega_\varphi - (L/K) * \omega_\theta = 0$

$$\omega_\varphi = \Delta\varphi / T_\theta$$

$$\omega_\theta = 2\pi / T_\theta$$

$$\text{or } L/K = (\omega - n * \omega_\varphi) / \omega_\theta$$

- Higher-order resonance (fractional resonance) has no effect on linear stability, but may have substantial effects for finite amplitude wave.

Constants of motion in toroidal plasmas (1)

- In axisymmetric (independent of toroidal angle φ) equilibrium (time-independent) fields:
 - energy E
 - magnetic moment μ
 - toroidal canonical momentum $P_\varphi = e_h \Psi + m_h R v_\varphi$ are constant along particle orbit
(Ψ is poloidal magnetic flux, e_h and m_h are charge and mass)

Constants of motion in toroidal plasmas (2)

- In the presence of a wave with angular frequency ω and toroidal mode number n :
 - μ is conserved if $\omega \ll \Omega_h = e_h B / m_h$
 - neither energy nor toroidal canonical momentum is conserved.
 - however, their combination $E' = E - \omega P_\phi / n$ is conserved.

E' is conserved during the wave-particle interaction in axisymmetric equilibrium (1)

Energy and toroidal momentum evolution with equilibrium field Hamiltonian H_0 and wave Hamiltonian H_1

$$\frac{dE}{dt} = \frac{\partial H}{\partial t} = \frac{\partial}{\partial t} (H_0 + H_1) = \frac{\partial}{\partial t} H_1$$

$$\frac{dP_j}{dt} = -\frac{\partial H}{\partial j} = -\frac{\partial}{\partial j} (H_0 + H_1) = -\frac{\partial}{\partial j} H_1$$

because $\frac{\partial}{\partial t} H_0 = 0$ (equilibrium)

and $\frac{\partial}{\partial j} H_0 = 0$ (axisymmetric).

E' is conserved during the wave-particle interaction in axisymmetric equilibrium (2)

Suppose the wave amplitude is constant,

H_1 is written in cylindrical coordinates (R, j, z)

$$H_1 = \hat{H}_1(R, z) e^{inj - i\omega t}$$

$$\frac{dE}{dt} = \frac{\partial H_1}{\partial t} = -i\omega \hat{H}_1(R, z) e^{inj - i\omega t}$$

$$\frac{dP_j}{dt} = -\frac{\partial H_1}{\partial j} = -in \hat{H}_1(R, z) e^{inj - i\omega t}$$

$$\text{Then, } \frac{dE}{dt} = \frac{d}{dt} \left(E - \frac{\omega}{n} P_j \right) = 0 \text{ is satisfied.}$$

Conservation of E' suggests ...

In wave - particle interaction in tokamak plasmas,
the conservation of E' leads to

$$\frac{dE}{W} = \frac{dP_j}{n} \gg \frac{e_h dy}{n}$$

Energy transfer between wave and particle (dE),
and change in poloidal magnetic flux (dy)
(= radial location; spatial transport) are related to each other.

This suggests qualitatively

for high W (such as ICRF): dE is important

for low W and high n (such as ITG): dy is important

Energy transfer, wave heating

Transport in radial direction

Why are AEs destabilized by energetic particles? (1)

Q1: Can particles interact with ideal MHD modes
with $E_{\parallel} = 0$?

A1: in toroidal plasmas, grad-B and curvature drifts
→ \mathbf{v}_{\perp} → energy transfer through $e_h \mathbf{v}_{\perp} \times \mathbf{E}_{\perp}$

Q2: Slowing down distribution and Maxwell
distribution have negative gradient in energy

$$\frac{\partial f}{\partial E} < 0$$

This leads to the stabilization of AEs due to Landau damping.

Why are AEs destabilized by energetic particles? (2)

We should consider the derivative

keeping $E' = E - \frac{W}{n} P_j = \text{constant}$,

$$\left. \frac{\partial f}{\partial E} \right|_{E'} = \frac{\partial f}{\partial E} + \frac{n}{W} \frac{\partial f}{\partial P_j}$$

The toroidal momentum is $P_j = e_n y + m_h R v_j$.

If we approximate $P_j @ e_n y$,

$$\frac{n}{W} \frac{\partial f}{\partial P_j} @ \frac{n}{W} \frac{\partial f}{\partial e_n y} = \frac{n}{W} \frac{1}{e_n R B_q} \frac{\partial f}{\partial r}$$

With $B_q = \frac{trB}{qR}$ ($B > 0$, $t = -1$ or 1)

$$\frac{n}{W} \frac{\partial f}{\partial P_j} @ \frac{n}{W} \frac{tq}{e_n B r} \frac{\partial f}{\partial r}$$

Why are AEs destabilized by energetic particles? (3)

Introducing "temperature" T which replaces energy derivative

$$\frac{\partial f}{\partial E} = -\frac{f}{T}, \text{ and } W_* = \frac{tqT}{e_n B} \frac{\partial \ln f}{r \partial r},$$

$$\left. \frac{\partial f}{\partial E} \right|_E = -\frac{f}{T} \left(1 - \frac{n}{W} W_* \right)$$

When the radial gradient of f is sufficiently large,

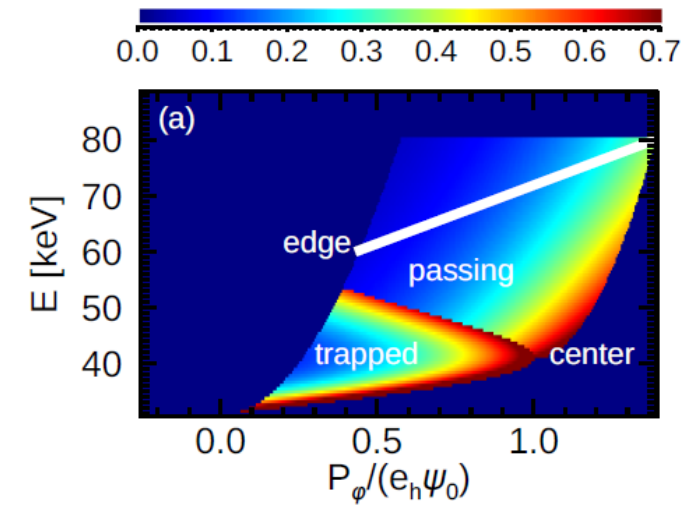
the second term $\frac{n}{W} W_*$ makes $\left. \frac{\partial f}{\partial E} \right|_E > 0$ to destabilize the AE.

This also determines the sign of n/W , i.e. the toroidal propagation

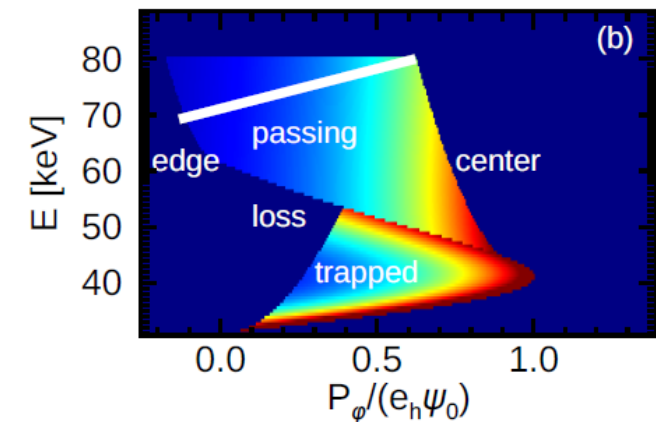
direction of the AE depending on the sign of $\frac{\partial f}{\partial r}$.

Why are AEs destabilized by energetic particles? (4)

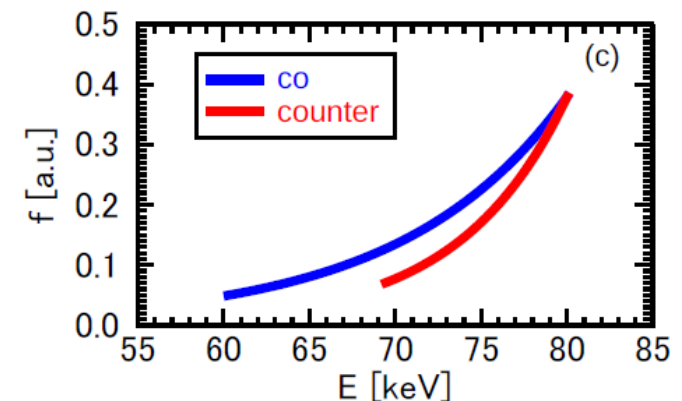
- Fast-ion distribution function in a tokamak plasma:
 $f(P_\phi, E)$, $\mu = \text{const.}$
- $R_0 = 1.8\text{m}$, $a = 0.6\text{m}$
- $B_0 = 2\text{T}$, $q_0 = 1.1$, $q_{\text{edge}} = 3.0$
- Deuterium, isotropic slowing-down distribution
- $E_b = 80\text{keV}$, $E_c = 30\text{keV}$
- $\text{Exp}[-P_\phi / 0.4\Psi_0]$
- White lines: $E' = \text{const}$
- AE with toroidal mode number $n=4$, $\text{freq.} = 70\text{kHz}$



Co



Counter



Why are AEs destabilized by energetic particles? (5)

For $n = 0$ modes, the energetic particle spatial gradient does not destabilize the AE modes.

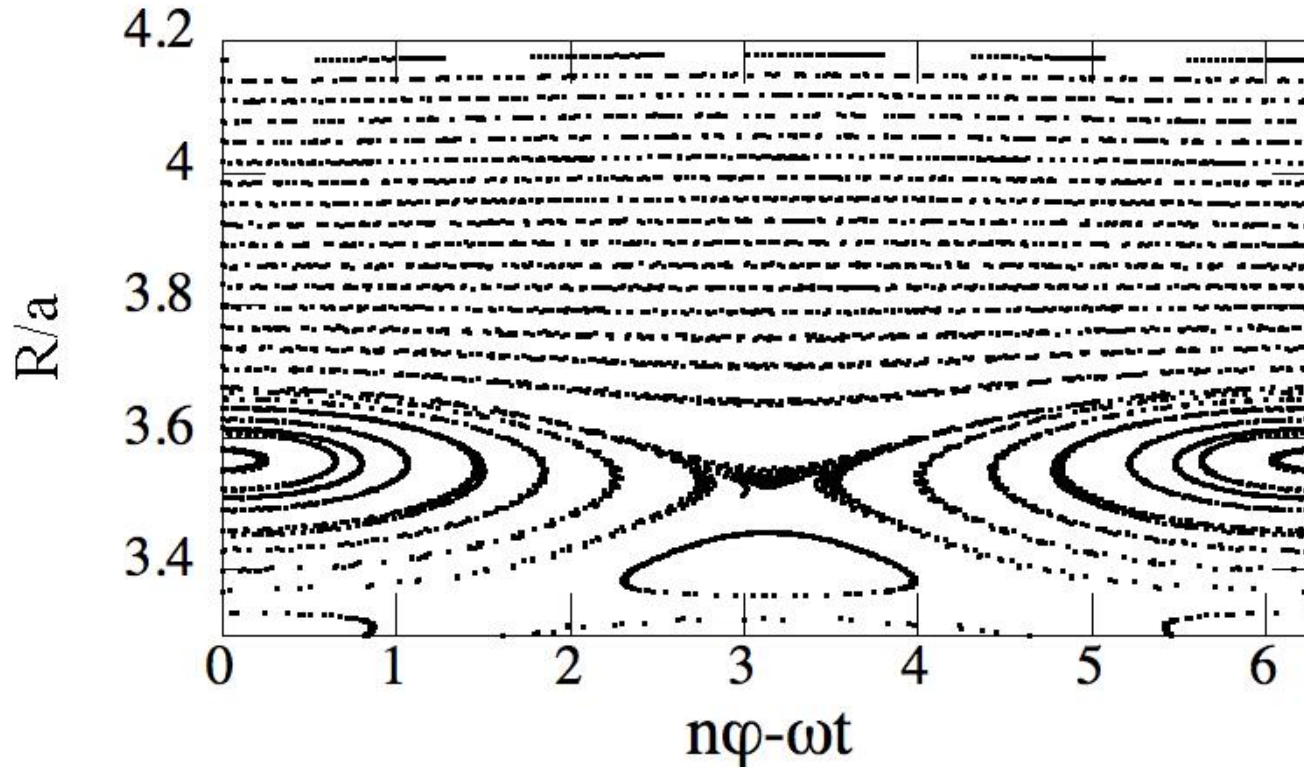
However, when f is not isotropic in velocity space and depends on pitch angle variable $\mathcal{L} = mB/E$, $f = f(E, \mathcal{L})$

$$\frac{\partial f}{\partial E} = \left. \frac{\partial f}{\partial E} \right|_{\mathcal{L}} + \frac{\partial \mathcal{L}}{\partial E} \left. \frac{\partial f}{\partial \mathcal{L}} \right|_E$$

The second term on the R.H.S. can lead to destabilization of $n = 0$ modes such as GAM.

EP PHASE SPACE STRUCTURE WITH AE

Poincaré plot of energetic-ion orbits in the presence of an AE with constant amplitude ($\delta B/B=2 \times 10^{-3}$ at the peak)



Particles have the same m and $E' = E - \frac{W}{n} P_j$.

[Todo+, Phys. Plasmas 10, 2888 (2003)]

- An island structure is formed in the phase space.
- This is the region of particles trapped by the AE.

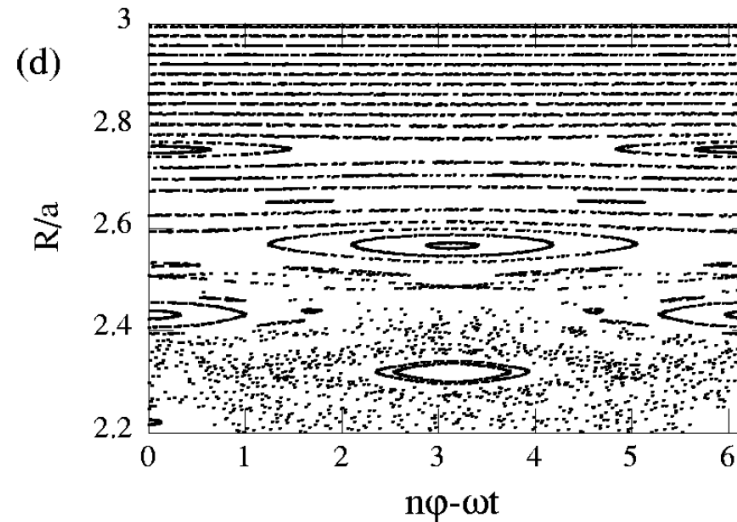
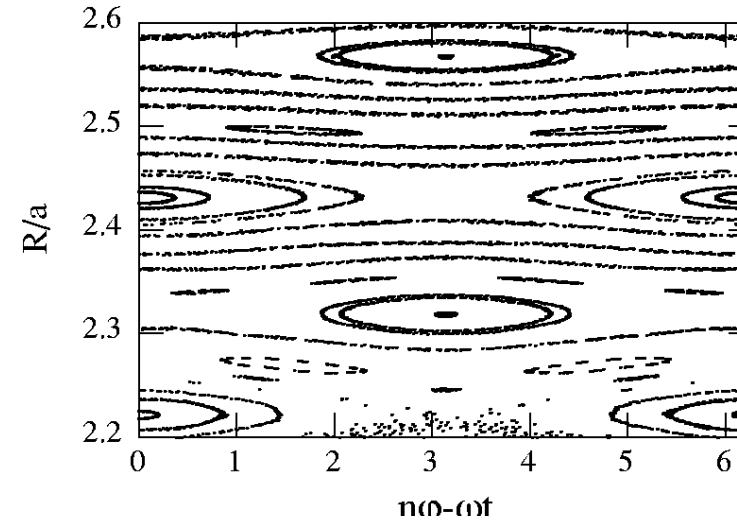
Higher-order islands and stochastic regions

$$n=3 \quad \delta B/B=8 \times 10^{-4}$$

many islands created by the higher-order resonances

$$n=3 \quad \delta B/B=2 \times 10^{-3}$$

KAM surfaces disappear due to the overlap of the higher-order islands



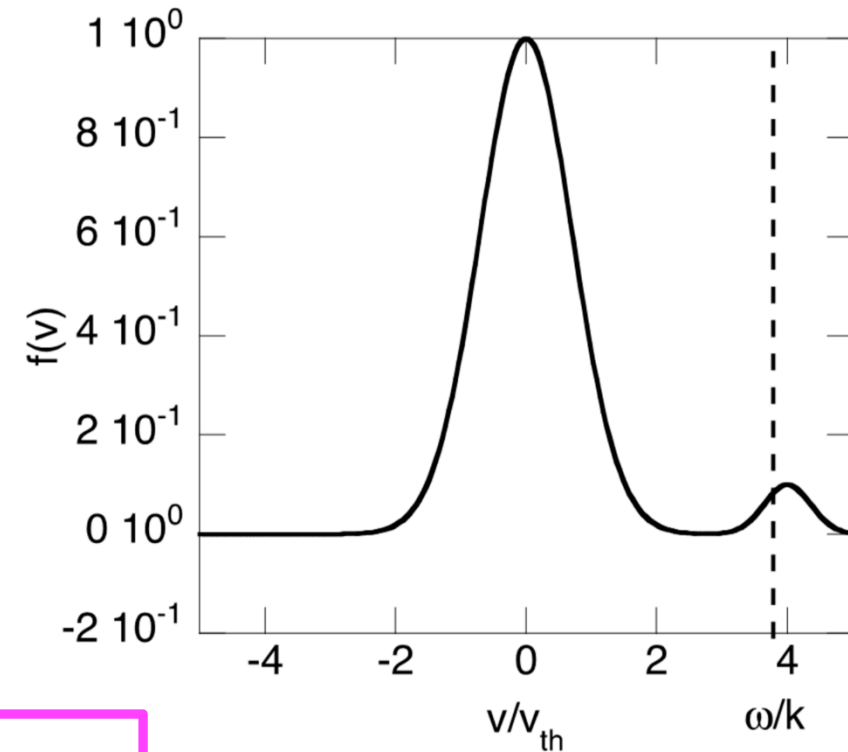
NONLINEAR EVOLUTION OF BUMP-ON-TAIL INSTABILITY AND FREQUENCY CHIRPING

Bump-on-tail instability

- 1-dimensional electrostatic model
- The bump in the high energy region leads to an inverse Landau damping

We consider

- Intrinsic wave damping (γ_d)
- Collision (ν) = effective source and sink



- It was expected that once the instability is saturated by particle trapping, the AE will damp monotonically in time with the intrinsic damping rate.
- However, the story was different when the AE is close to the marginal stability ...

Berk, Breizman, Pekker, PRL **76**, 1256 (1996)

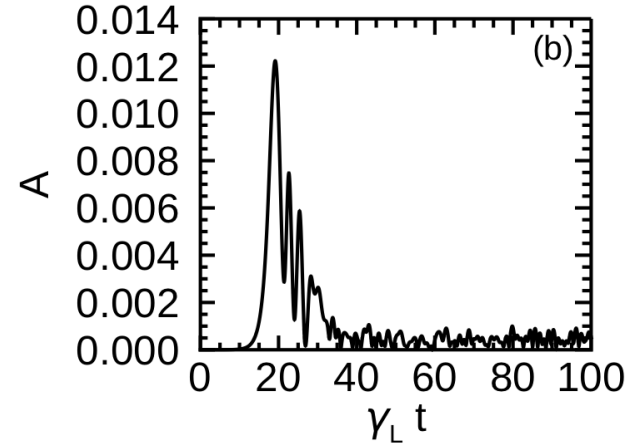
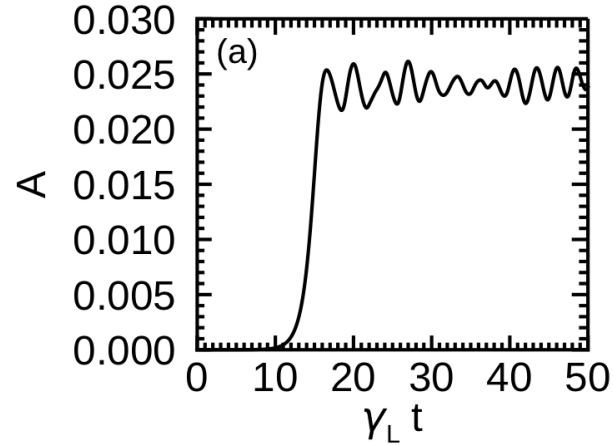
Berk, Breizman, Petviashvili, Phys. Lett. A **234**, 213 (1997), **238**, 408(E) (1998)

Berk et al., Phys. Plasmas 6, 3102 (1999)

Various types of time evolution of wave amplitude (1-dimensional simulation of bump-on-tail instability)

$\gamma_d = 0, \nu = 0$

particle trapping

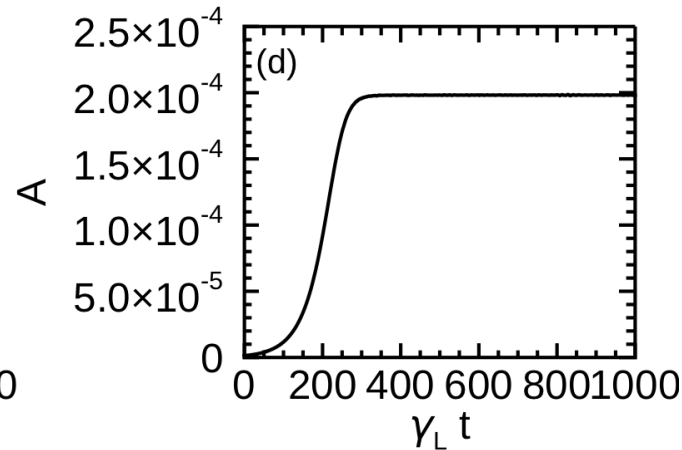
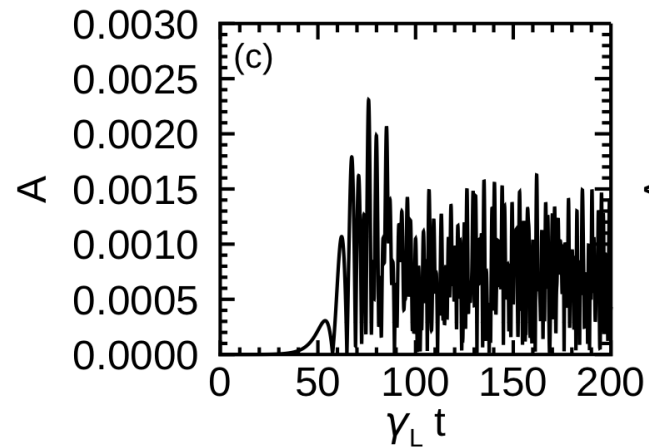


$\gamma_L \gg \gamma_d, \nu = 0$

damping

$\gamma_L \sim \gamma_d, \nu = 0$

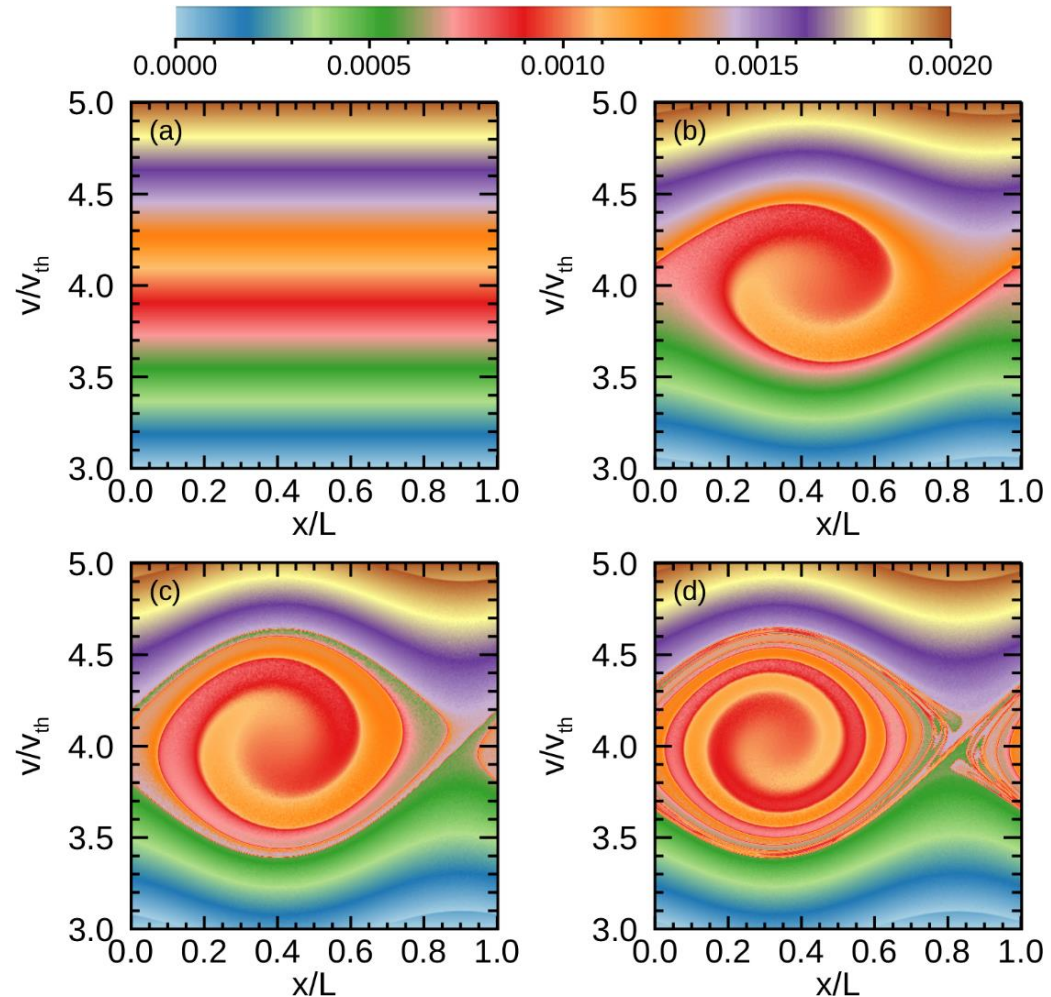
frequency chirping



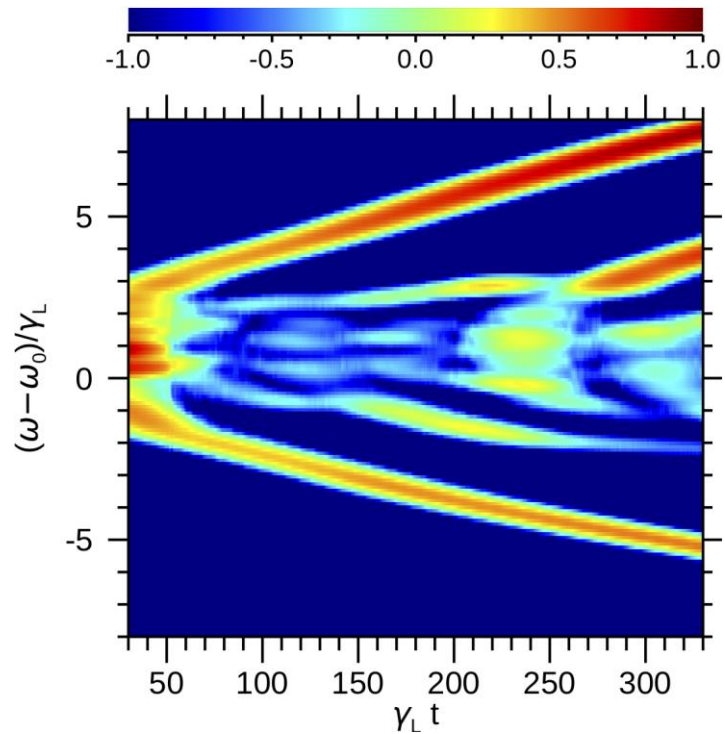
$\nu \gg \gamma_L - \gamma_d,$

steady state

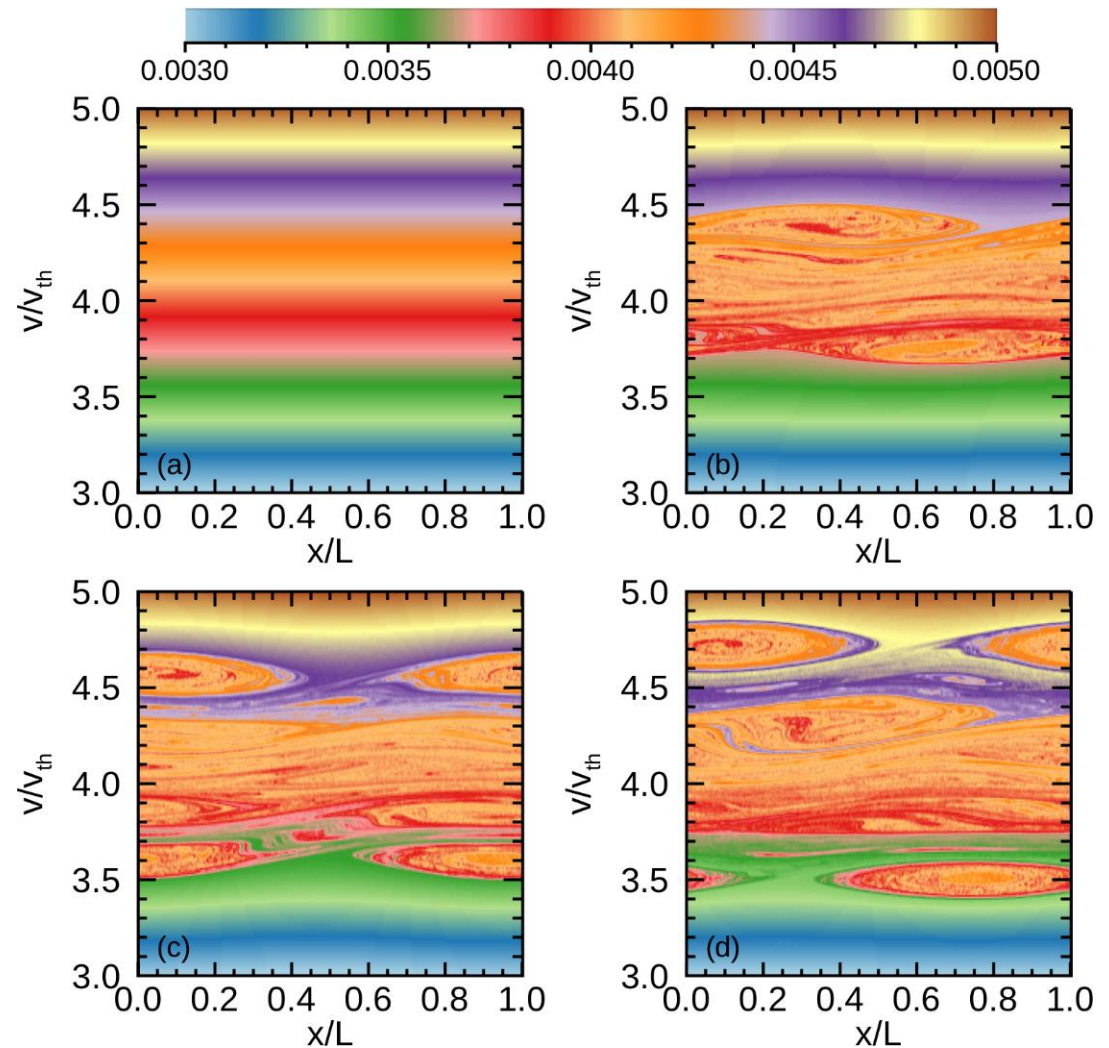
Distribution function evolution ($\gamma_d=0$, $\nu=0$, particle trapping)



$\gamma_L \sim \gamma_d, \nu=0$ frequency chirping



Frequency spectrum evolution

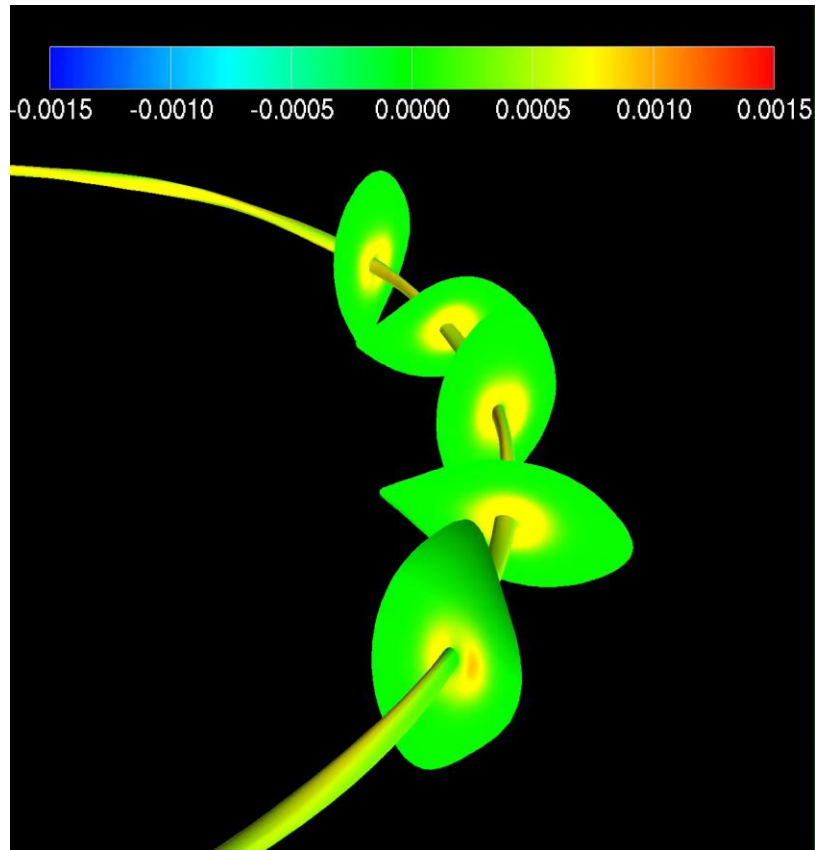


Distribution function evolution

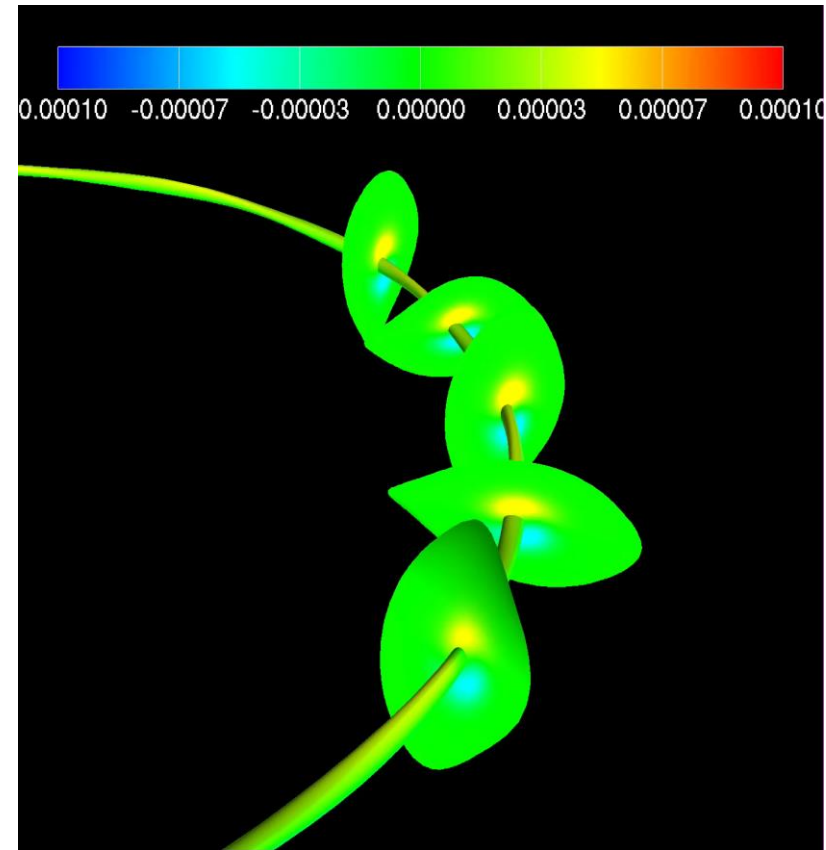
Explanation of frequency chirping

- Hole and clump are BGK modes.
- The structure of hole/clump and the frequency shift should be consistent with each other.
- The energy release due to the frequency chirping is balanced with the mode damping.

Simulation of energetic particle driven geodesic acoustic mode (EGAM) in LHD



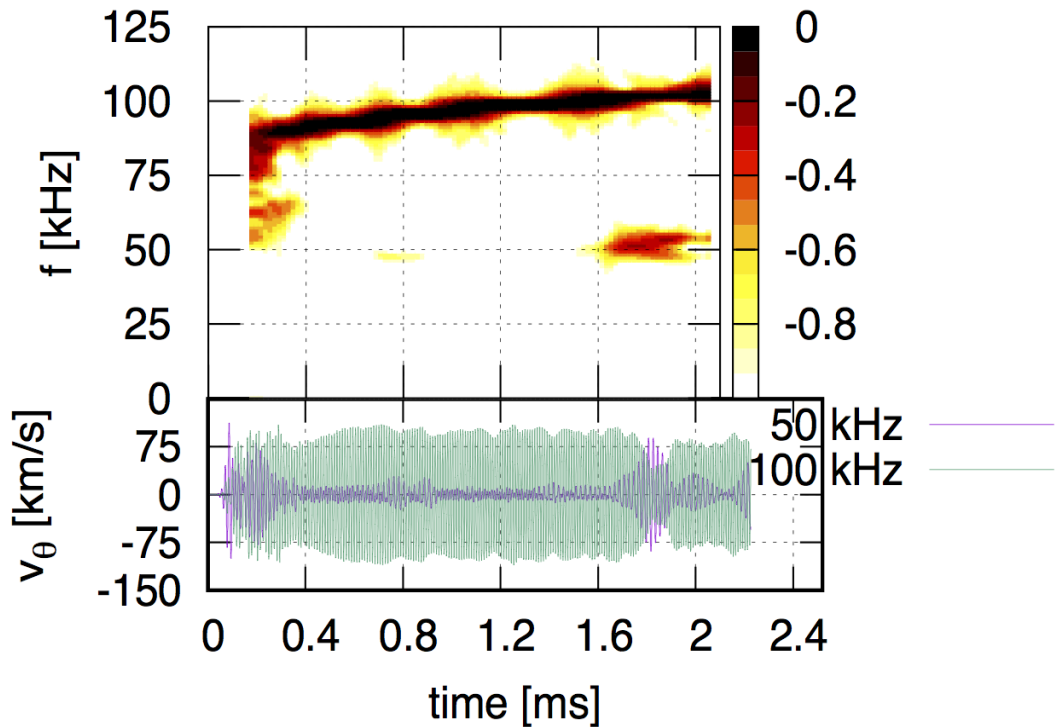
MHD velocity



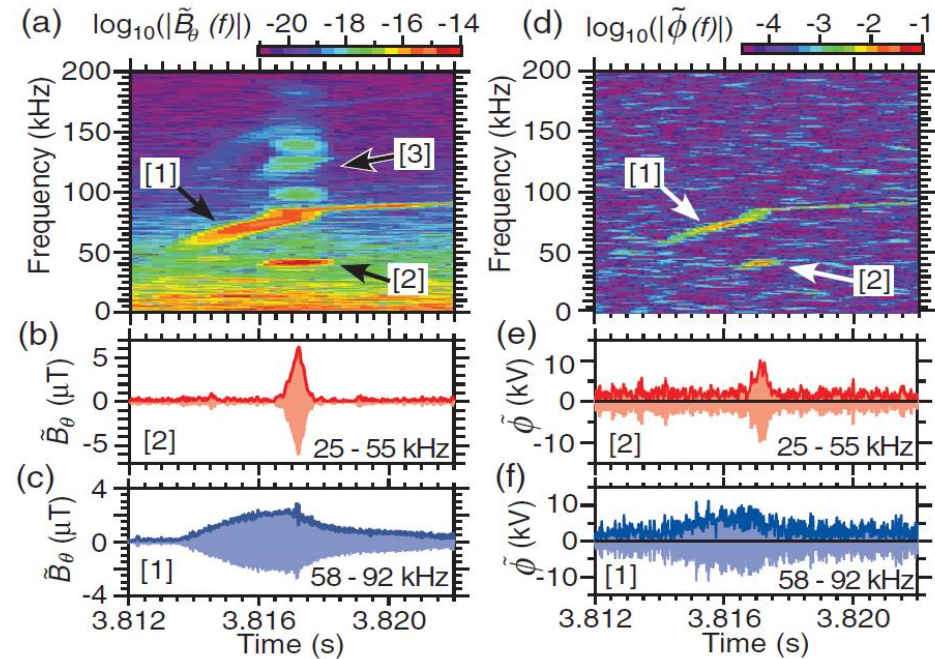
Plasma pressure



Frequency chirping and sudden excitation of a half-frequency mode are reproduced by kinetic-MHD simulation



Simulation



LHD experiment
 [T. Ido et al., PRL (2016),
 M. Lesur et al., PRL (2016)]

[H. Wang et al., PRL **120**, 175001 (2018)]

KINETIC-MHD HYBRID SIMULATION

Initial value codes for the interaction between AEs and energetic particles

Method	AE modes	EP	Advantages	Codes
Kinetic-MHD hybrid simulation	MHD eq.	computational particles (or Vlasov eq. or gyrofluid eq.)	nonlinear MHD effects	M3D-C1 FAR3D HMGC HYMAGYC MEGA XTOR-K HYM
Reduced simulation	AEs given by linear analysis	computational particles	computationally less demanding	ORBIT HAGIS CKA-EUTERPE MEGA-R
Gyrokinetic simulation	computational particles for bulk plasma + GK Poisson eq. and Ampere eq.	computational particles (or Vlasov eq.)	fully kinetic effects	GTC ORB5 EUTERPE GEM GYRO GYSELA

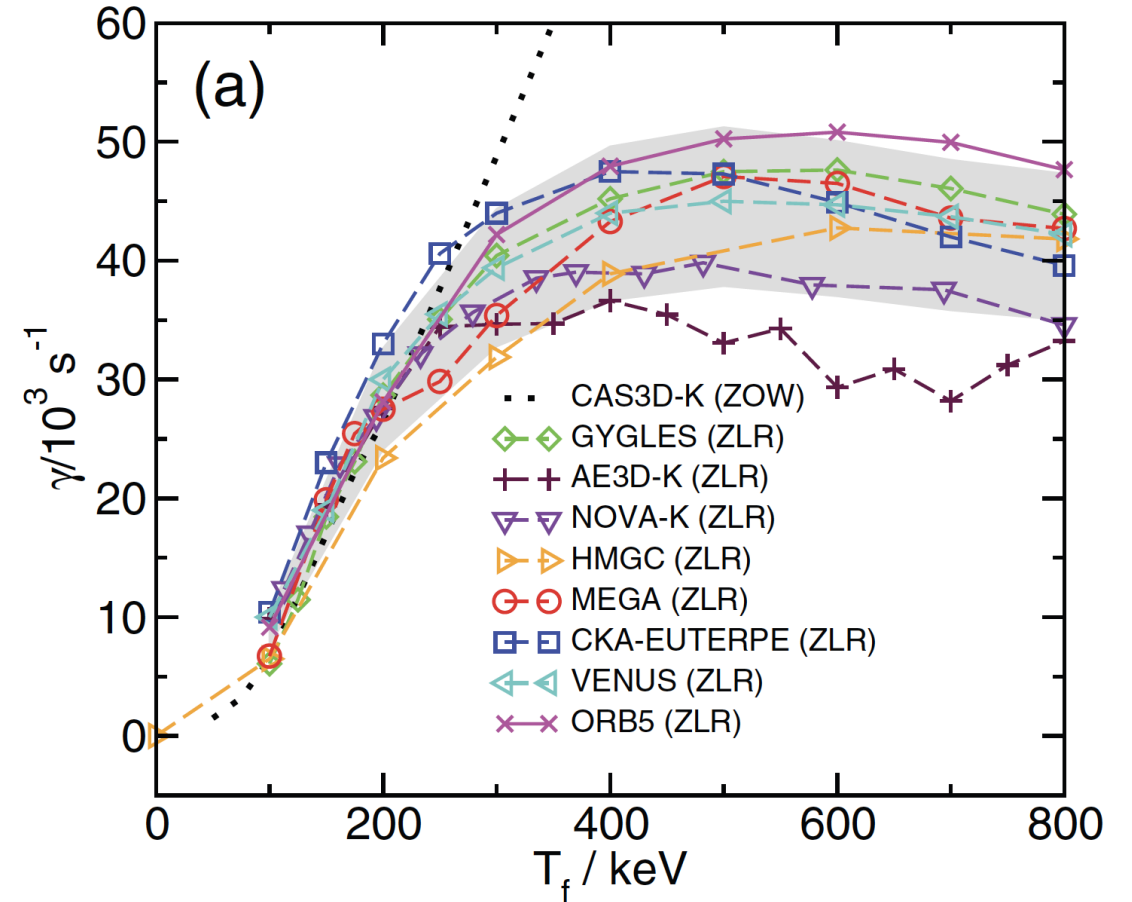
Can MHD model AEs correctly?

- Comparison in electron temperature fluctuation profile between MHD analysis (NOVA) and experiment on DIII-D [Van Zeeland (NF 2009)].
- “It is found that ideal MHD modelling of eigenmode spectral evolution, coupling and structure are in excellent agreement with experimental measurements.”
- => MHD is fine to model AEs !

M.A. Van Zeeland et al.,
Nuclear Fusion **49**, 065003 (2009)
Fig. 3

Verification between MHD and GK on AEs

- “A linear benchmark for a toroidal Alfvén eigenmode (TAE) is done with 11 participating codes with a broad variation in the physical as well as the numerical models.”
[Könies (NF 2018)]
- A reasonable agreement of around 20% has been found for the growth rates.
- Another benchmark work was also conducted by Taimourzadeh (NF 2019).



A. Könies et al.,
Nuclear Fusion **58**, 126027 (2018)

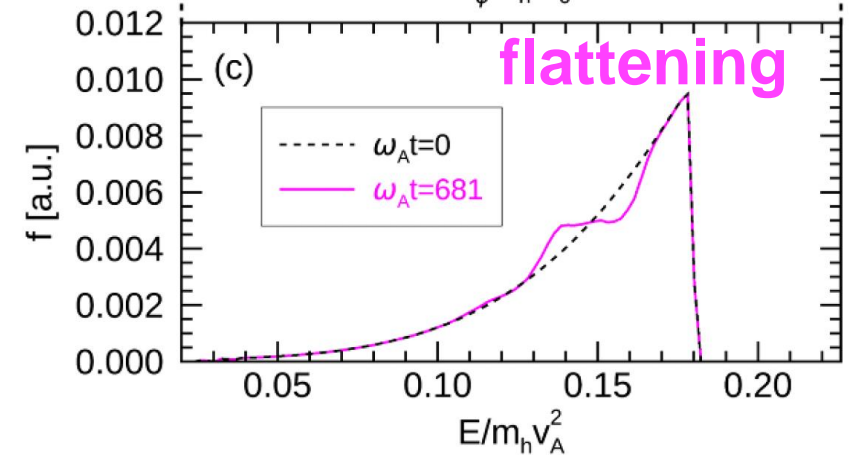
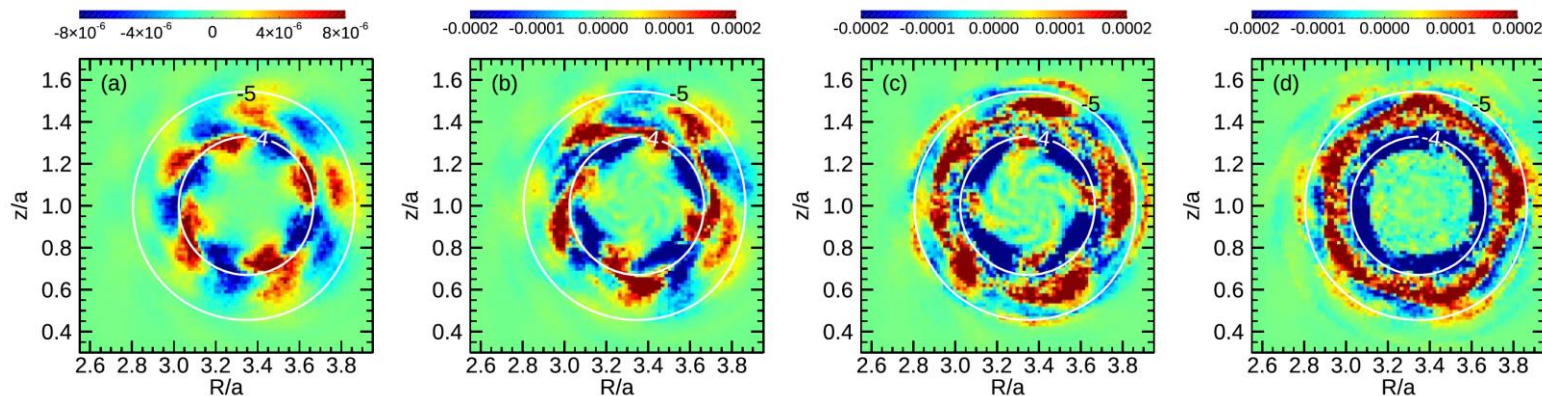
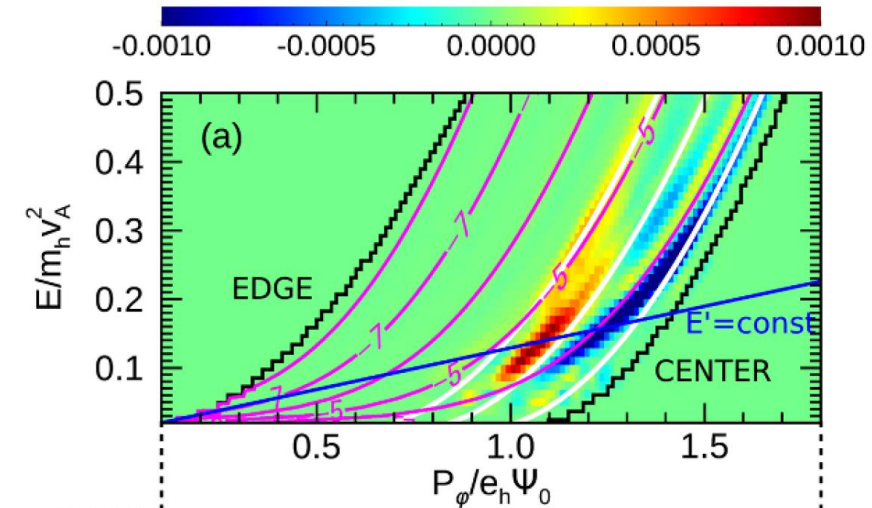
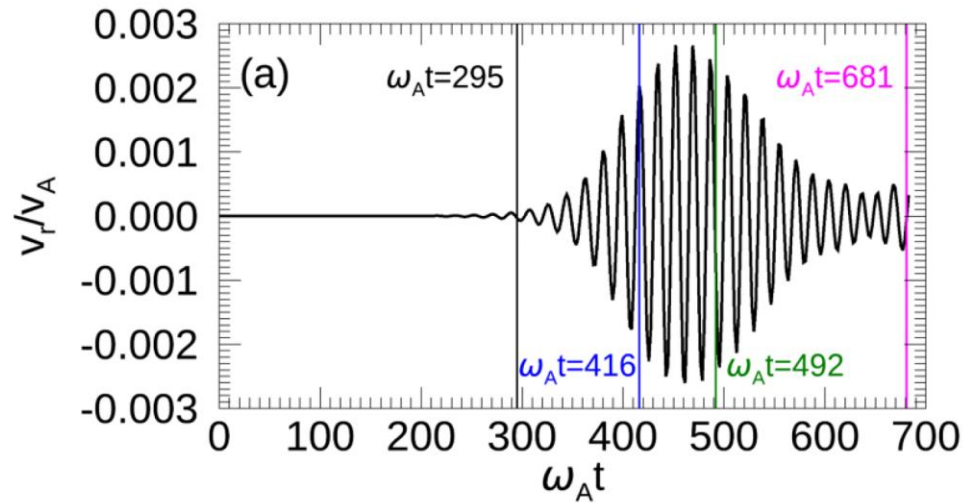
MEGA:

Hybrid simulation for energetic particles and MHD

- energetic particles (fast ions, alphas, energetic electrons): gyrokinetic particle-in-cell (PIC) simulation
- bulk plasma: MHD simulation
- the coupling between EP and MHD is taken into account through the EP current in the MHD momentum equation
- **Extensions:**
 - **neutral beam injection (NBI), collisions, ICRF**
 - **multi-phase simulation** for fast ion distribution formation process in the slowing-down time scale
 - **kinetic thermal ions**

A single AE evolution and flattening of fast ion distribution function

(top L) evolution of AE
 (bottom L) fast ion DF on a poloidal plane (R, z)
 (top R) fast ion DF in (P_φ, E) plane
 (bottom R) fast ion DF along an E'=const. line



NONLINEAR MHD EFFECTS AND ZF GENERATION

Y. Todo et al., Nucl. Fusion **50** (2010) 084016

Y. Todo et al., Nucl. Fusion **52** (2012) 094018

Comparison between linear and NL MHD runs (\mathbf{j}_h ' is restricted to $n=4$)

$$\frac{\partial r}{\partial t} = -\nabla \cdot (r_{\text{eq}} \mathbf{v}) + n_n D(r - r_{\text{eq}})$$

$$r_{\text{eq}} \frac{\partial}{\partial t} \mathbf{v} = -\nabla p + (\mathbf{j}_{\text{eq}} - \mathbf{j}'_{\text{heq}}) \times \mathbf{B} + (d\mathbf{j} - d\mathbf{j}'_h) \times \mathbf{B}_{\text{eq}}$$

$$+ \frac{4}{3} \nabla (nr_{\text{eq}} \nabla \cdot \mathbf{v}) - \nabla \times (nr_{\text{eq}} \mathbf{w})$$

$$\frac{\partial \mathbf{B}}{\partial t} = -\nabla \times \mathbf{E}$$

$$\frac{\partial p}{\partial t} = -\nabla \cdot (p_{\text{eq}} \mathbf{v}) - (g-1) p_{\text{eq}} \nabla \cdot \mathbf{v} + n_n D(p - p_{\text{eq}})$$

$$+ h d\mathbf{j} \cdot \mathbf{j}_{\text{eq}}$$

$$\mathbf{E} = -\mathbf{v} \times \mathbf{B}_{\text{eq}} + h(\mathbf{j} - \mathbf{j}_{\text{eq}})$$

$$\mathbf{j} = \frac{1}{m_0} \nabla \times \mathbf{B}$$

$$\mathbf{w} = \nabla \times \mathbf{v}$$

$$\frac{\partial r}{\partial t} = -\nabla \cdot (r\mathbf{v}) + n_n D(r - r_{\text{eq}})$$

$$r \frac{\partial}{\partial t} \mathbf{v} = -r\mathbf{w} \times \mathbf{v} - r\nabla \left(\frac{v^2}{2} \right) - \nabla p + (\mathbf{j} - \mathbf{j}'_h) \times \mathbf{B}$$

$$+ \frac{4}{3} \nabla (nr \nabla \cdot \mathbf{v}) - \nabla \times (nr\mathbf{w})$$

$$\frac{\partial \mathbf{B}}{\partial t} = -\nabla \times \mathbf{E}$$

$$\frac{\partial p}{\partial t} = -\nabla \cdot (p\mathbf{v}) - (g-1) p \nabla \cdot \mathbf{v} + n_n D(p - p_{\text{eq}})$$

$$+ (g-1) \left[nrw^2 + \frac{4}{3} nr(\nabla \cdot \mathbf{v})^2 + h\mathbf{j} \cdot (\mathbf{j} - \mathbf{j}_{\text{eq}}) \right]$$

$$\mathbf{E} = -\mathbf{v} \times \mathbf{B} + h(\mathbf{j} - \mathbf{j}_{\text{eq}})$$

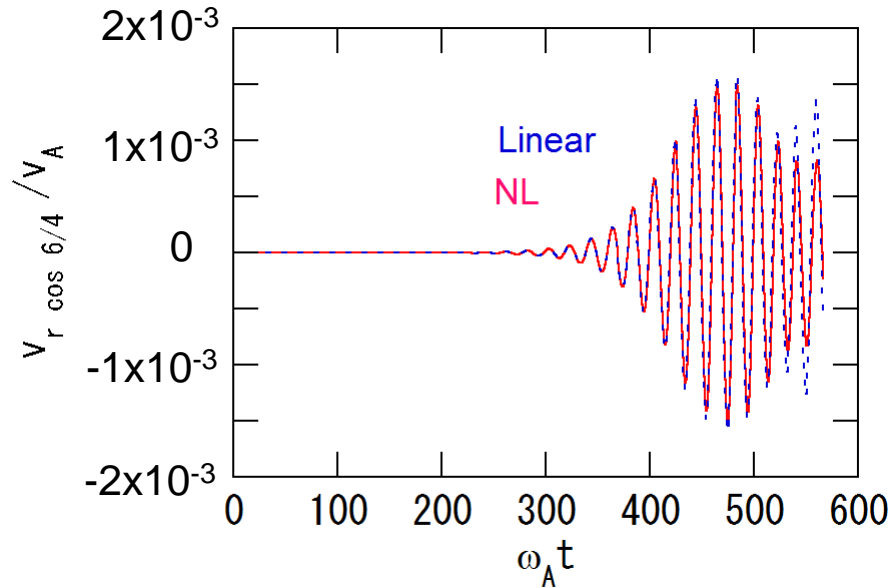
$$\mathbf{j} = \frac{1}{m_0} \nabla \times \mathbf{B}$$

$$\mathbf{w} = \nabla \times \mathbf{v}$$

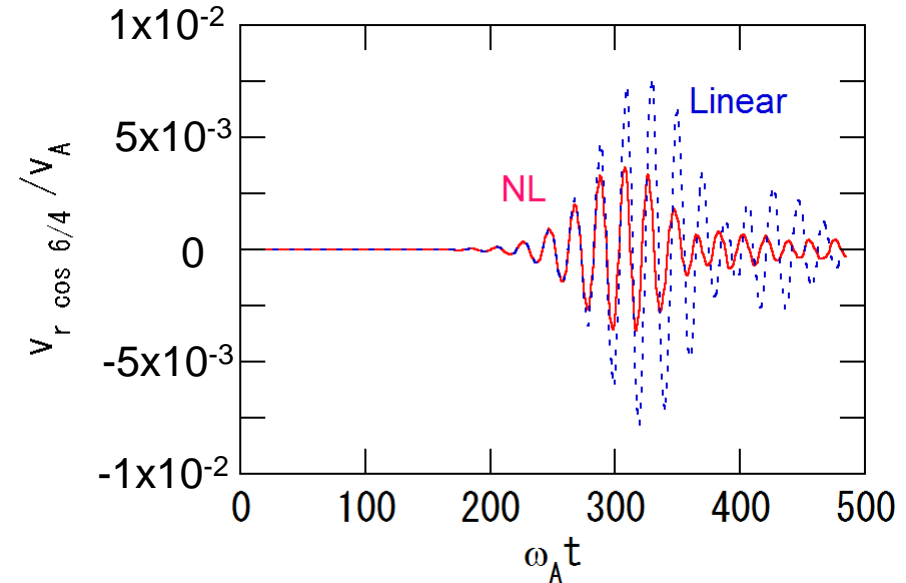
↑
EP effects

The viscosity and resistivity are $\nu = \nu_n = 2 \times 10^{-7} v_A R_0$ and $\eta = 2 \times 10^{-7} \mu_0 v_A R_0$.
The numbers of grid points are (128, 64, 128) for (R, ϕ , z).
The number of marker particles is 5.2×10^5 .

Nonlinear MHD effect on AE saturation level



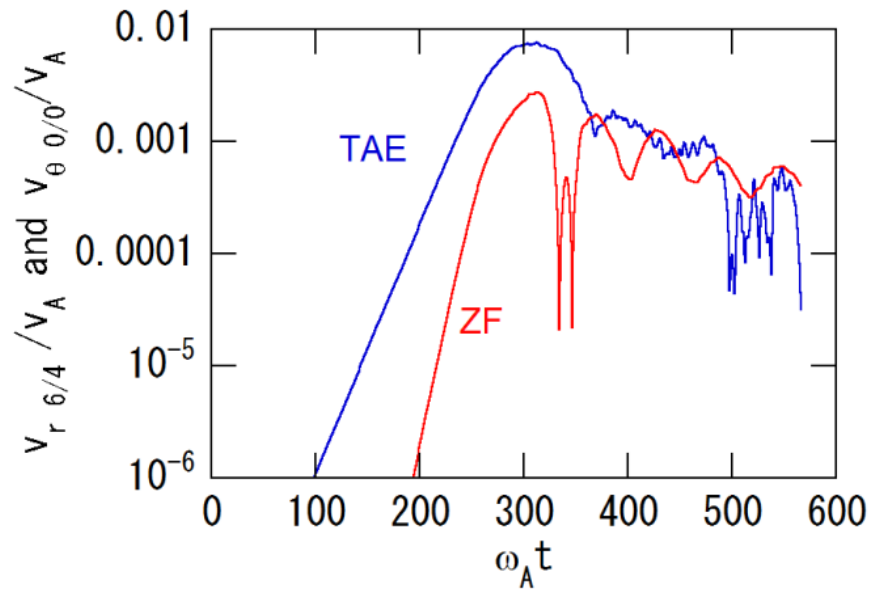
$\beta_{h0}=1.5\%$
Sat. Level (linear) $\sim 1.5 \times 10^{-3}$
Sat. Level (NL) $\sim 1.5 \times 10^{-3}$



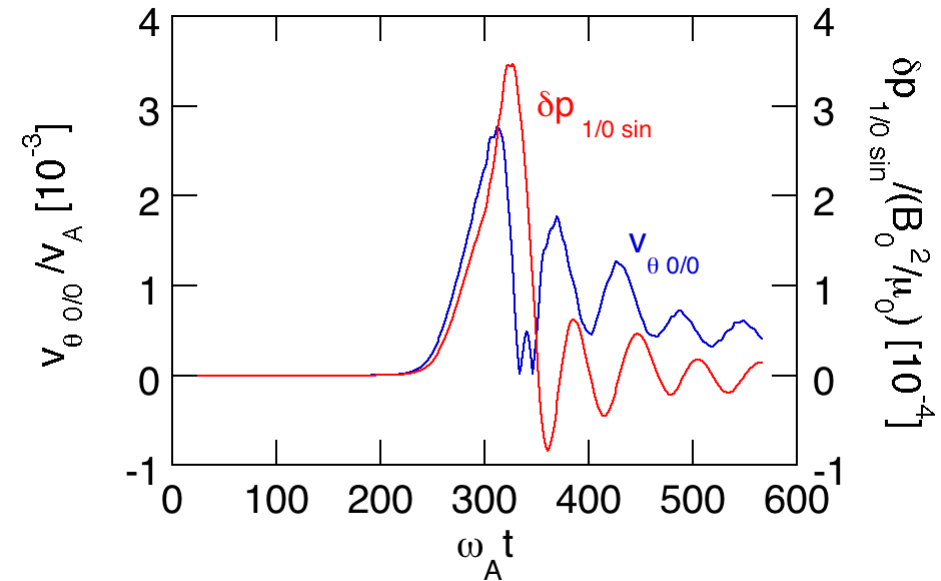
$\beta_{h0}=2.0\%$
Sat. Level (linear) $\sim 8 \times 10^{-3}$
Sat. Level (NL) $\sim 4 \times 10^{-3}$

The saturation level is reduced to half by the nonlinear MHD effect.

ZF Evolution and GAM Excitation

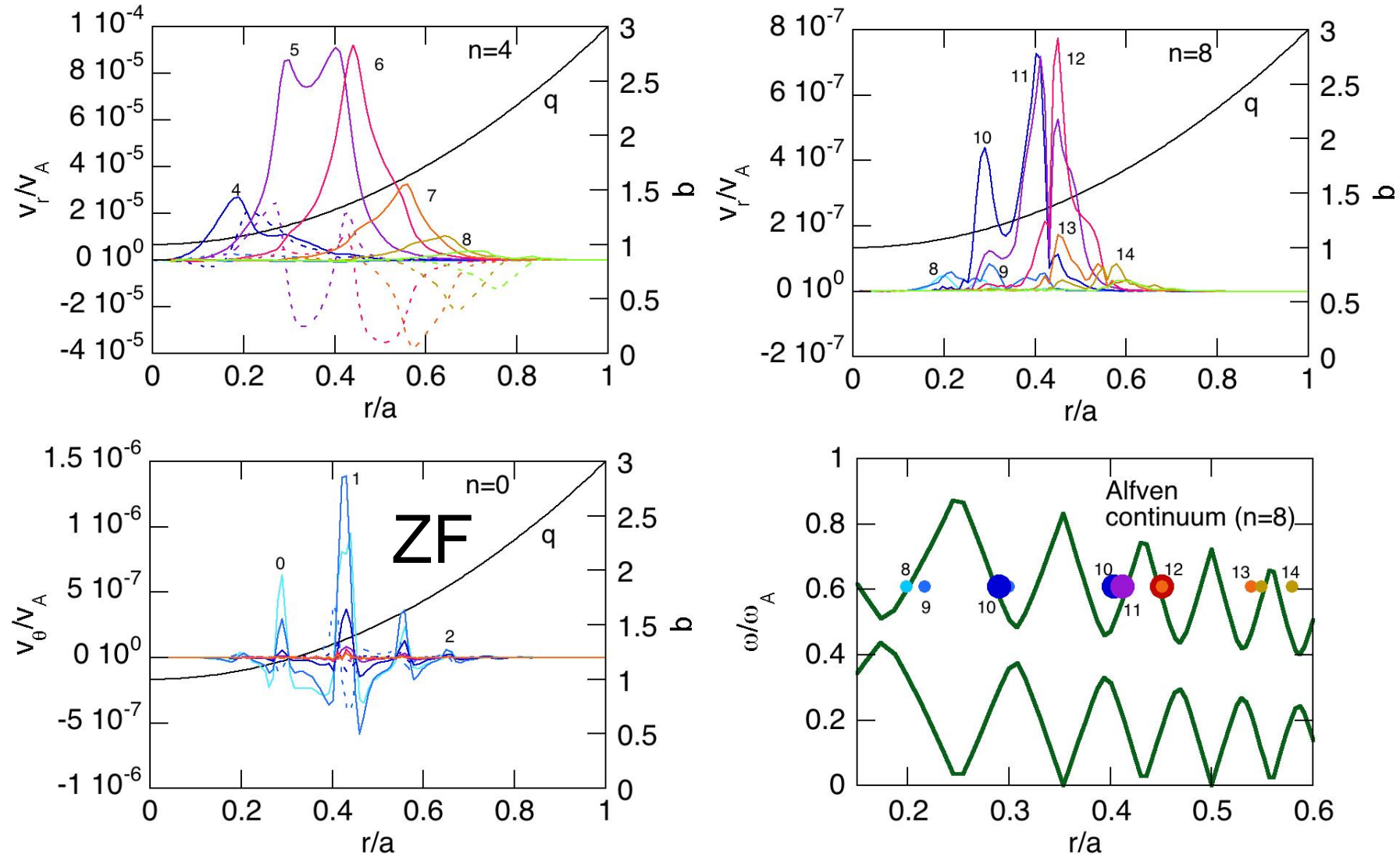


Evolution of TAE and zonal flow. The growth rate of ZF is twice that of the TAE.

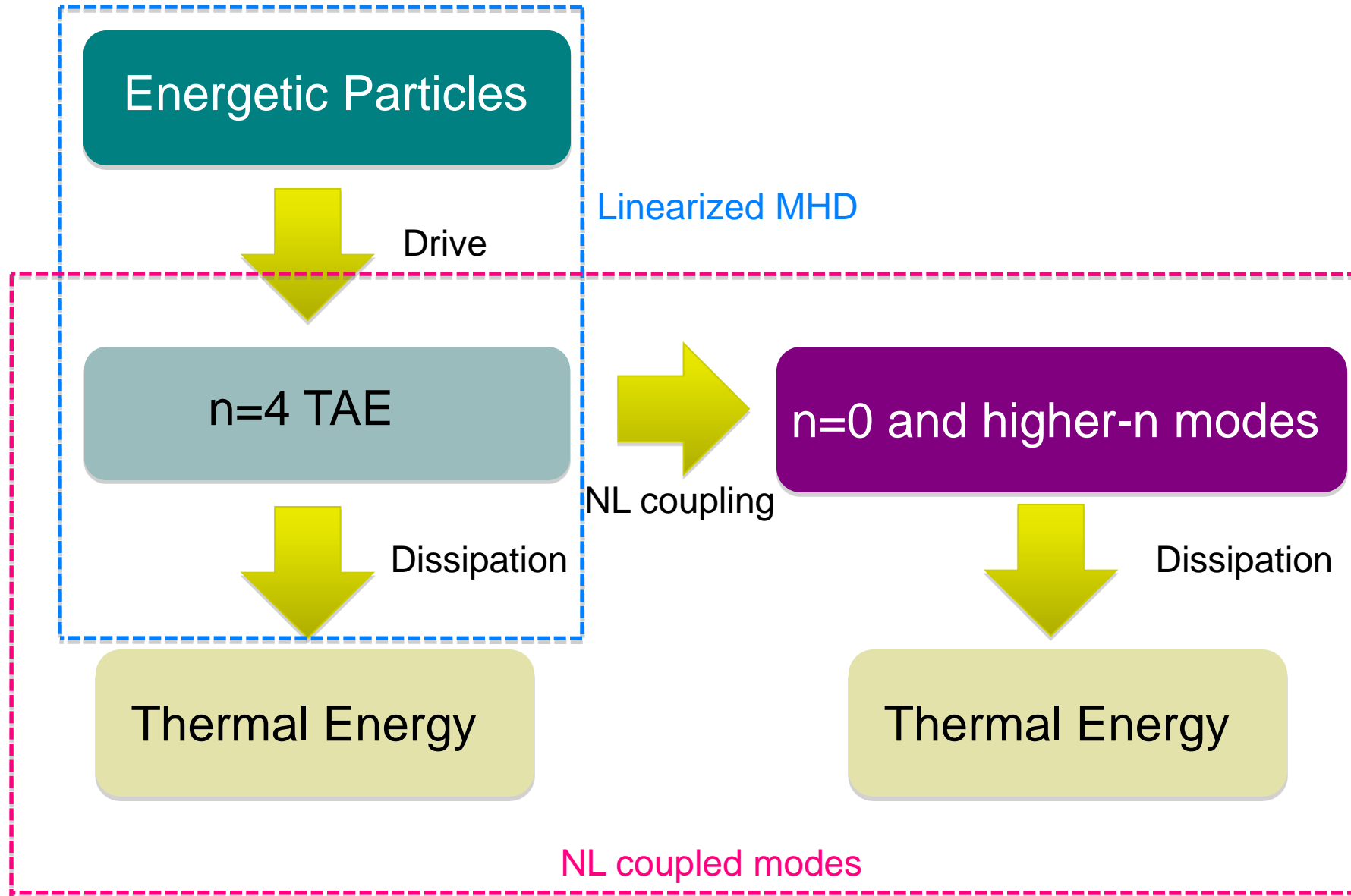


After the saturation of the TAE instability, a **geodesic acoustic mode (GAM)** is excited.

Spatial profiles of the TAE and NL modes: Evidence for continuum damping of the higher-n (n=8) mode



Schematic Diagram of Energy Transfer



FAST ION PROFILE FLATTENING AND STIFFNESS IN DIII-D EXPERIMENTS

Y. Todo et al., Nucl. Fusion **54** (2014) 104012

Y. Todo et al., Nucl. Fusion **55** (2015) 073020

Y. Todo et al., Nucl. Fusion **56** (2016) 112008

Anomalous Flattening of Fast ion Profile on DIII-D

Fig. 1

Fig. 3

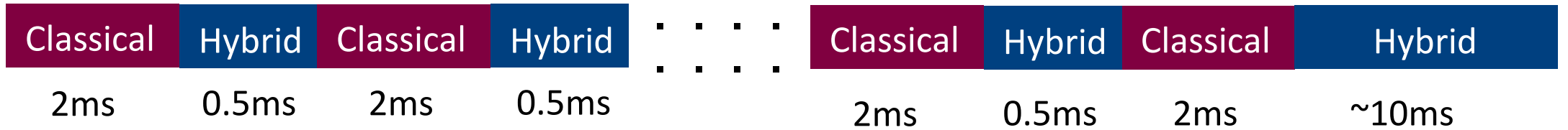


[W. W. Heidbrink, PRL **99**, 245002 (2007)]

- Anomalous flattening of the fast-ion profile during Alfvén-eigenmode activity
- A rich spectrum of TAEs and RSAEs with reversed q profile in current ramp-up phase

Multi-phase Simulation

[Y. Todo, Nucl. Fusion 54, 104012 (2014)]

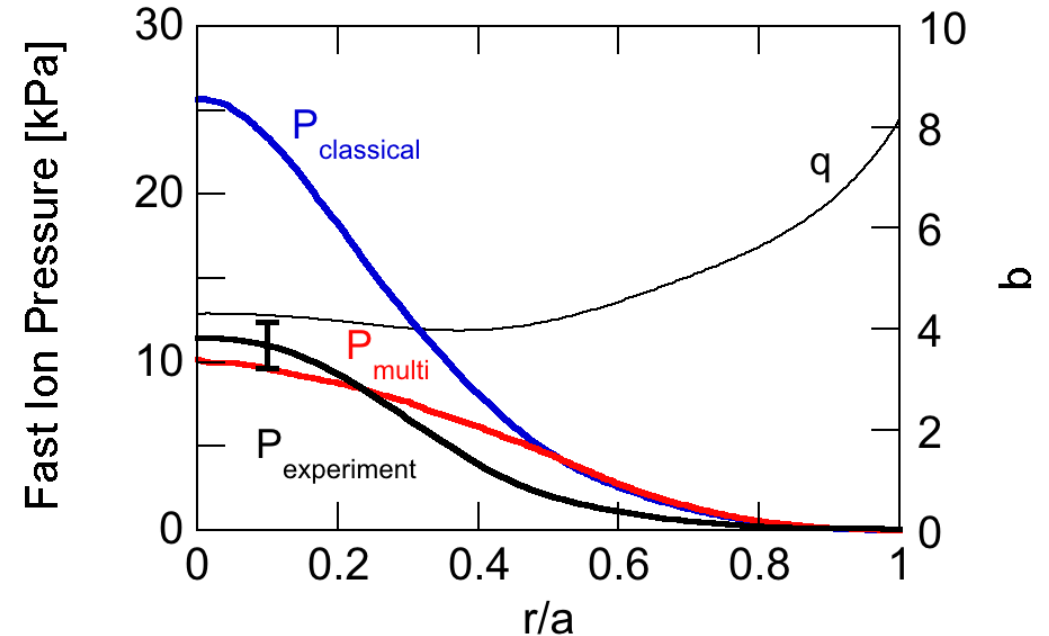


until a steady state or
a limit cycle appears

- Hybrid simulation of energetic particles and an MHD fluid
- Multi-phase simulation =
 - classical simulation w/o MHD perturbations for 2ms +
 - EP-MHD hybrid simulation for 0.5ms; performed alternately
 - reduce computational time to 1/5

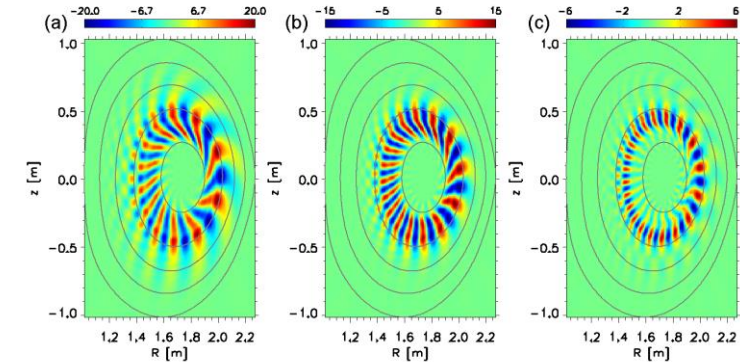
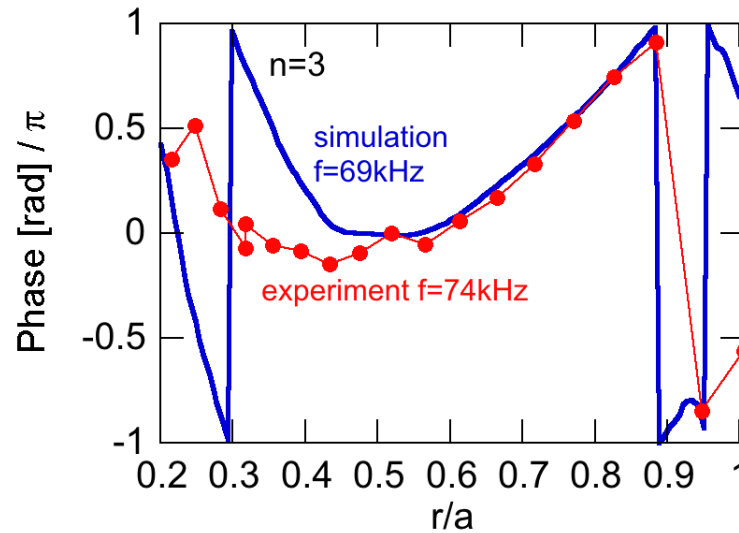
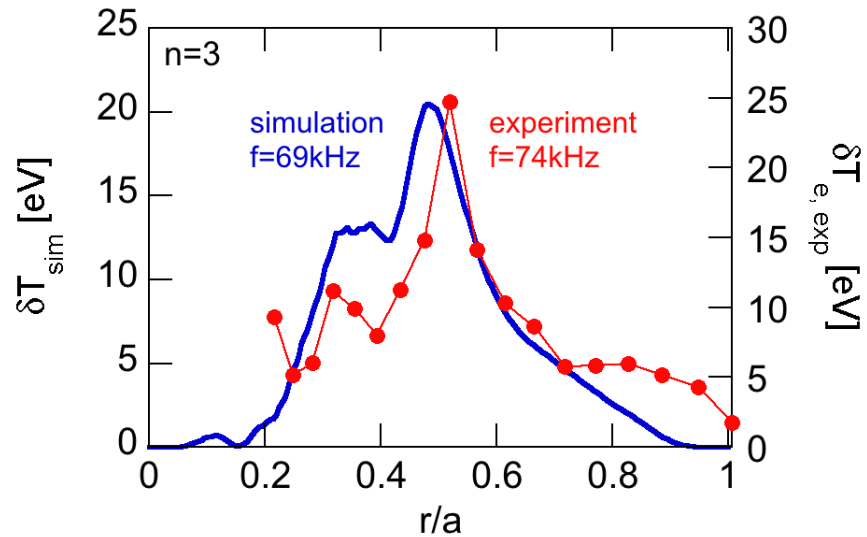
Comparison of fast ion pressure profiles (classical, multi-phase, exp.)

- Fast ion pressure profile flattening takes place in the multi phase simulation.
- The fast pressure profile in the multi-phase simulation is close to that in the experiment.



[Y. Todo et al., NF **55**, 073020 (2015)]

Comparison of temperature fluctuation profile with ECE measurement for n=3

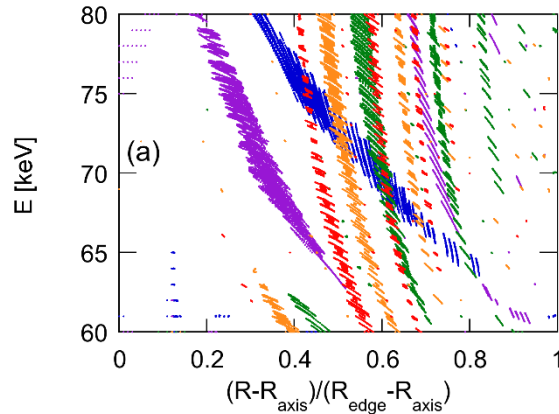


[Y. Todo et al., NF 55, 073020 (2015)]

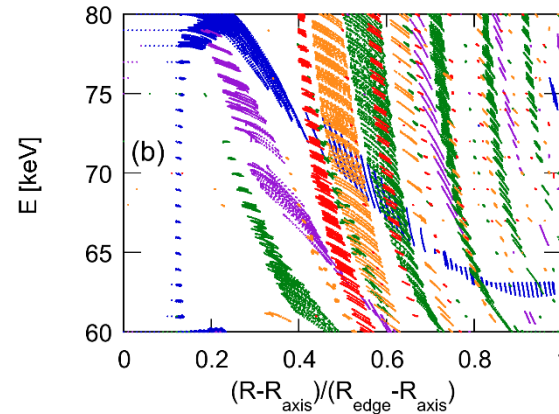
- good agreement in spatial profile
- good agreement in **absolute amplitude**
- good agreement in phase profile

Resonance overlap in (R,E) phase space [blue (n=1), purple (n=2), green (n=3), orange (n=4), red(n=5)]

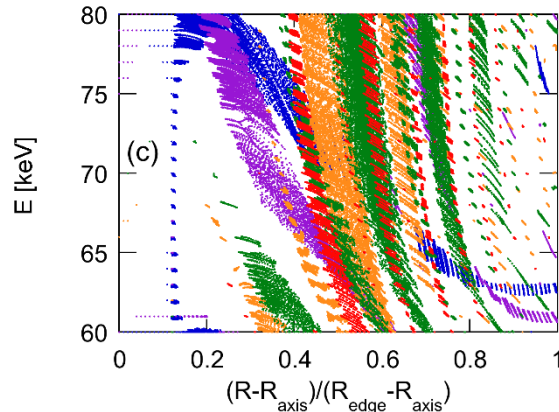
$P_{\text{NBI}}=1.56\text{MW}$



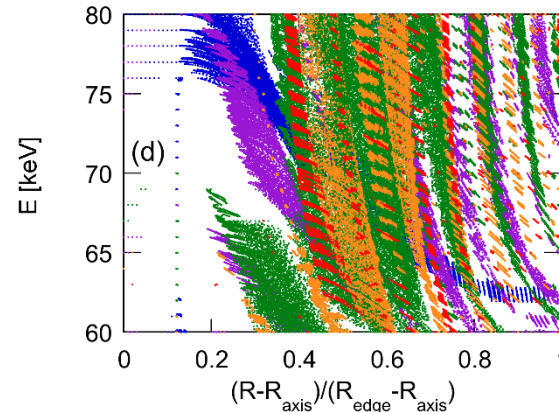
$P_{\text{NBI}}=3.13\text{MW}$



$P_{\text{NBI}}=6.25\text{MW}$



$P_{\text{NBI}}=15.6\text{MW}$



Phase space regions trapped by AEs (=resonances).

With increasing beam power [(a)->(d)], the resonance overlap covers the phase space.

AE BURSTS & STEADY EVOLUTION, DEPENDENCE ON P_{NBI} AND SLOWING DOWN TIME

Y. Todo, New J. Physics **18**, 115005 (2016)

Y. Todo, Nucl. Fusion **59**, 096048 (2019)

Alfvén Eigenmode Bursts in TFTR

Results from a TFTR experiment
[K. L. Wong et al., PRL **66**, 1874 (1991)]

Fig. 4

Neutron emission:

nuclear reaction of thermal D and beam D
-> drop in neutron emission = fast ion loss

Mirnov coil signal:

magnetic field fluctuation
-> Alfvén eigenmode bursts

- Alfvén eigenmode bursts take place with a roughly constant time interval.
- 5-7% of energetic beam ions are lost at each burst.

AE Bursts have been observed in many tokamaks and stellarators/heliotrons

- tokamaks

- DIII-D [Heidbrink+ NF1991]
- JT-60U [Kusama+ NF1999]
- NSTX [Fredrickson+ PoP2006]
- MAST [Gryaznevich+ NF2006]

- stellarators/heliotrons

- CHS/LHD [Toi+ NF2000]
- W-7AS [Weller+ PoP2001]
- TJ-II [Jiménez-Gómez+, NF2011]
- Heliotron J [Yamamoto+ NF2017]

Fig. 9

Multiple AEs

AE bursts in LHD
[Osakabe+, NF 46, S911 (2006)]

Resonance overlap of multiple modes; evolution of bump-on-tail instability with two waves

Stairway
distribution

Fig. 7

Fig. 6

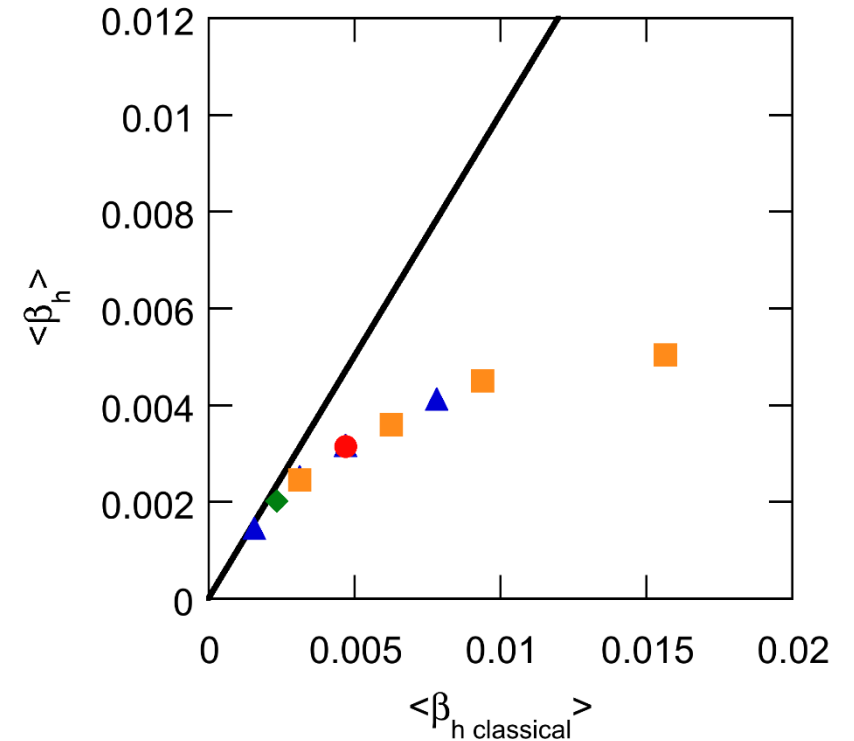
(top) EP distribution function for different moments with two waves.

(bottom) Time evolution of the total wave energy.

[Berk, Breizman et al., Phys. Plasmas **2**, 3007 (1995)]

Objective

- Apply the multi-phase hybrid simulation to a tokamak plasma similar to the TFTR experiment for various beam power and slowing down time
 - time evolution (steady, intermittent, time interval of bursts)
 - maximum amplitude
 - degradation of fast ion confinement
 - fast ion profile resiliency (saturation of fast ion pressure profile)
- Investigate the physical process of the AE bursts



Fast ion confinement degrades for higher classical fast ion beta. [Y. Todo, New J. Phys. **18**, 115005 (2016)]

Simulation condition based on the TFTR experiment

- $R_0=2.4\text{m}$, $a=0.75\text{m}$, $B_0=1\text{T}$
- beam injection energy 110keV (deuterium)
- $n_i=2.8 \times 10^{19} \text{ m}^{-3}$ (deuterium)
- $q(r) = 1.2 + 1.8(r/a)^2$
- beam deposition profile:
 $\exp[-(r/0.4a)^2] \times \exp[-(|\lambda|-\lambda_0)^2/\Delta\lambda^2]$

$$\lambda=v_{//}/v, \lambda_0=0.7, \Delta\lambda=0.3$$

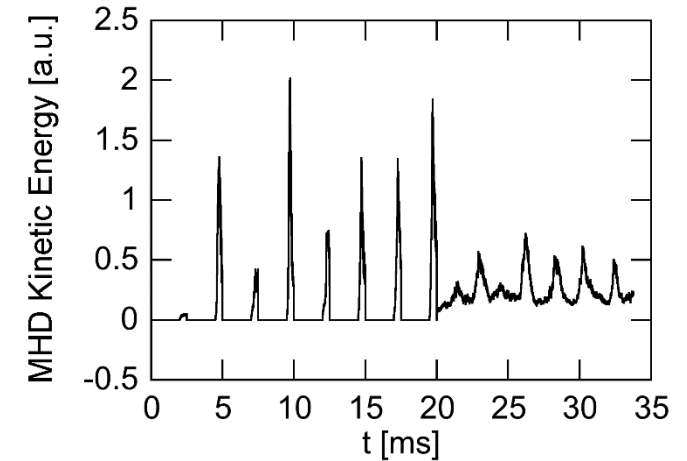
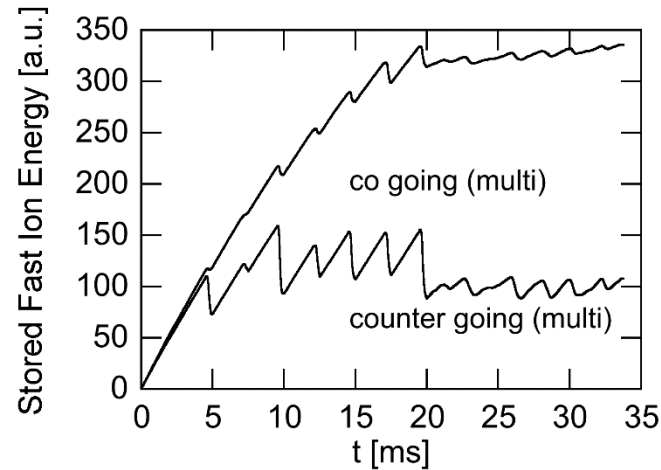
- slowing down & pitch-angle scattering

$$v_d=(1/2)v_s (v_c/v)^3$$

$P_{\text{NBI}}=10\text{MW}$, $\tau_s=100\text{ms}$ (similar to the TFTR experiment)

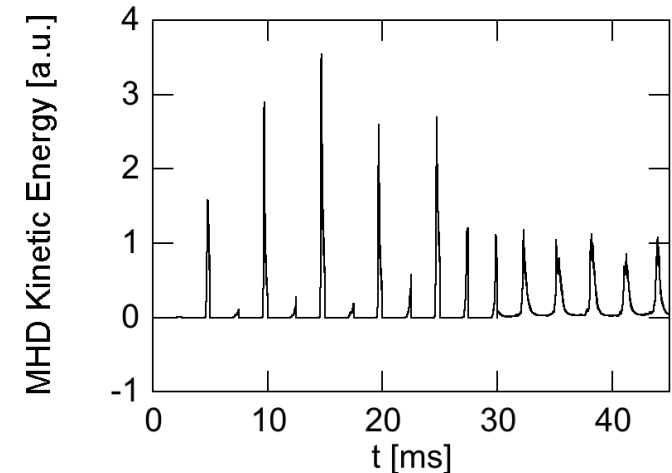
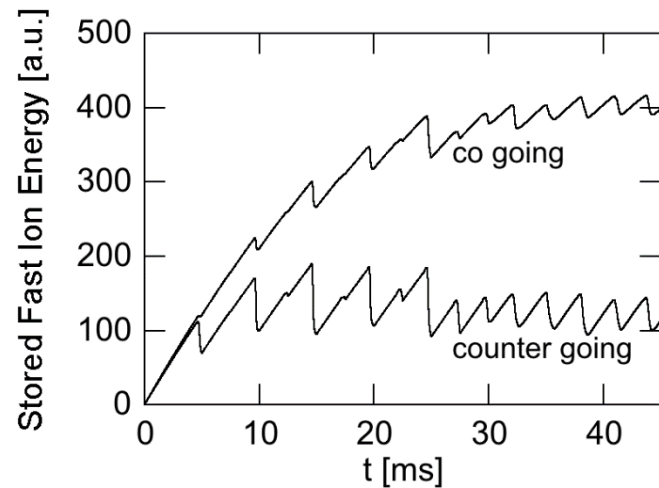
4.2M particles

[Y. Todo, New J. Phys. 2016]

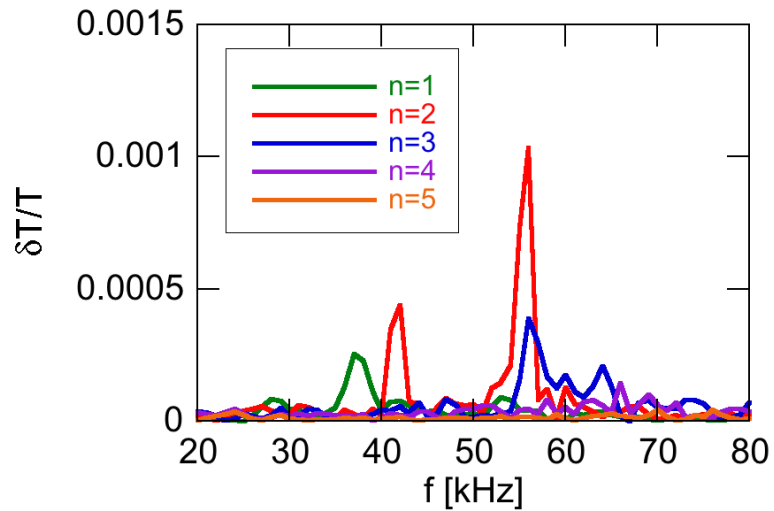


for distribution function
analysis -> 67M particles

- Good convergence in number of particles
- Reduced numerical noise

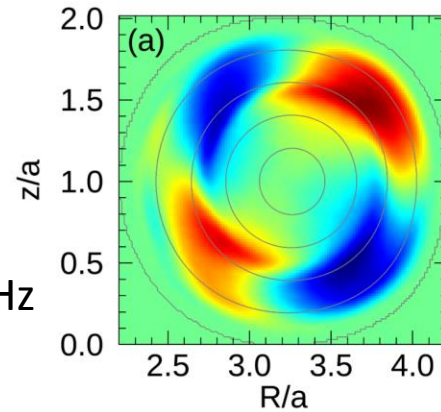


Frequency spectra and spatial profiles of AEs

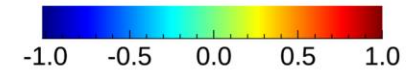


- AEs with $n=1-5$ are destabilized.
- The largest amplitude modes are $n=1-3$.
- The $n=1$ mode is an EPM, and the others are TAE.

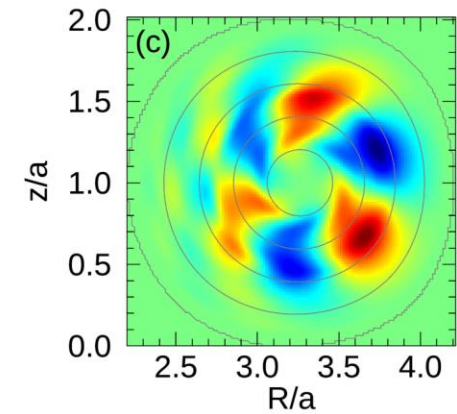
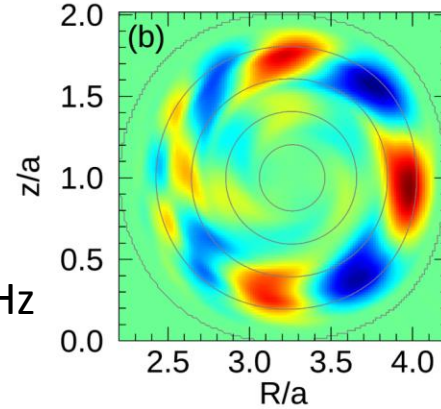
$n=1$, 37kHz



Toroidal electric field (E_ϕ) in an (R, z) plane for each spectrum peak

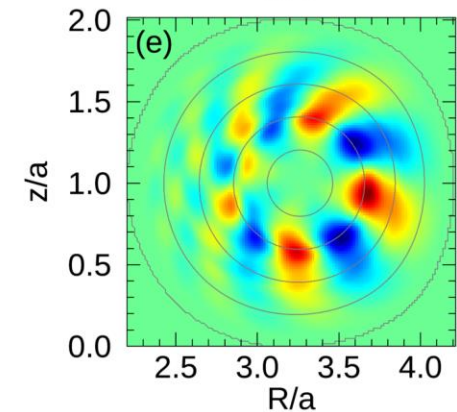
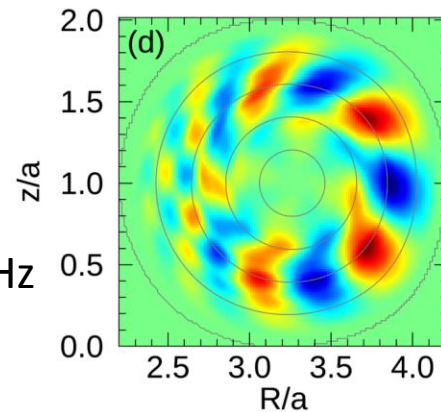


$n=2$, 42kHz



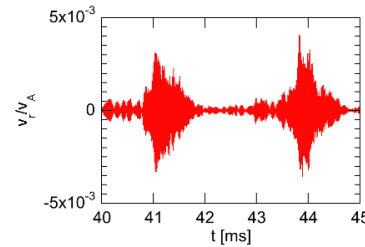
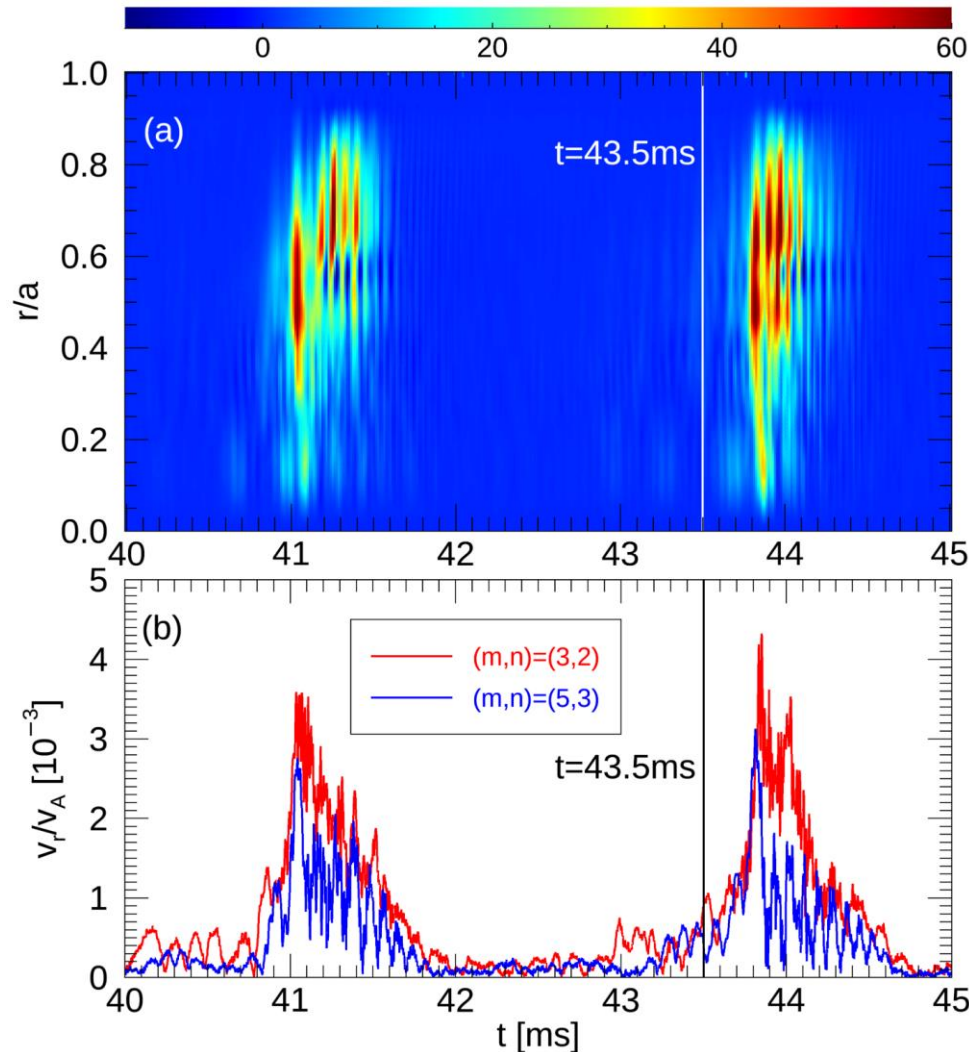
$n=2$, 56kHz

$n=3$, 56kHz

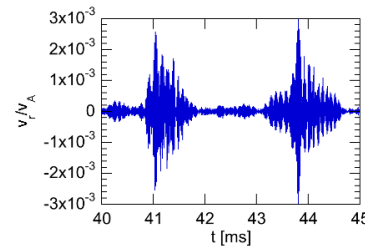


$n=3$, 64kHz

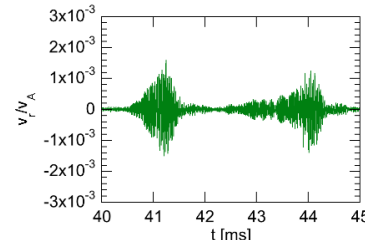
Synchronization of multiple AEs and fast ion energy flux profile evolution



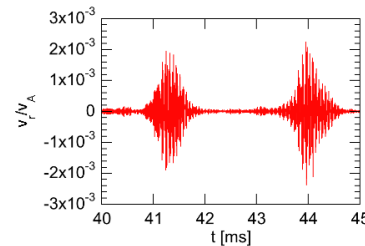
$m/n=3/2$



$m/n=5/3$



$m/n=2/1$

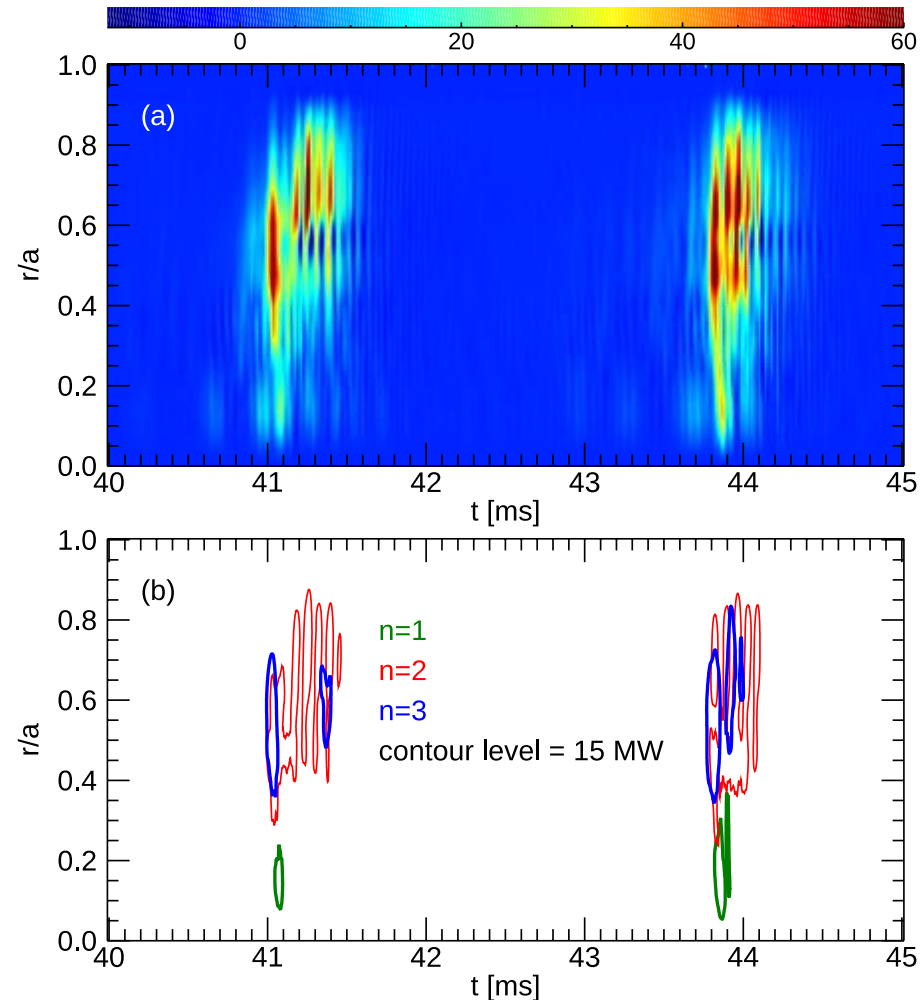
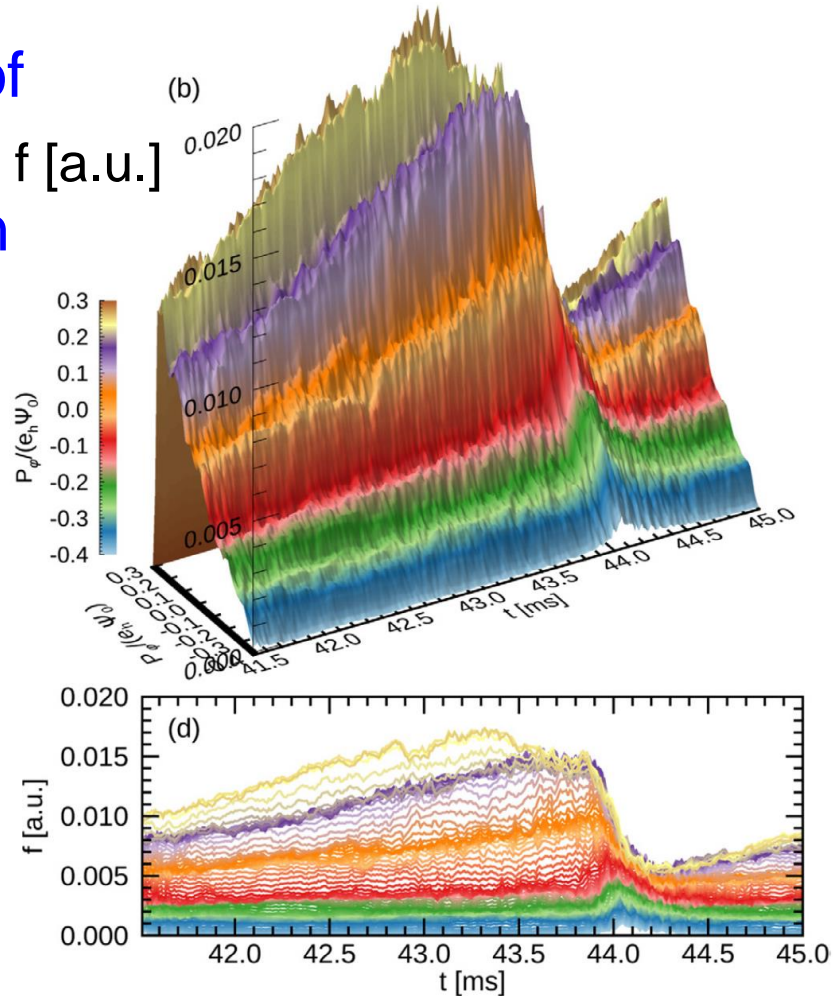


$m/n=4/2$

- Synchronization of multiple AEs.
- Time interval of the bursts is ~ 3 ms.
- Maximum amplitude is $v/v_A \sim 3 \times 10^{-3}$.
=> close to the TFTR experiment.
- Energy flux ~ 60 MW (NBI 10MW)
- Focus on the **distribution function at $t=43.5$ ms.**

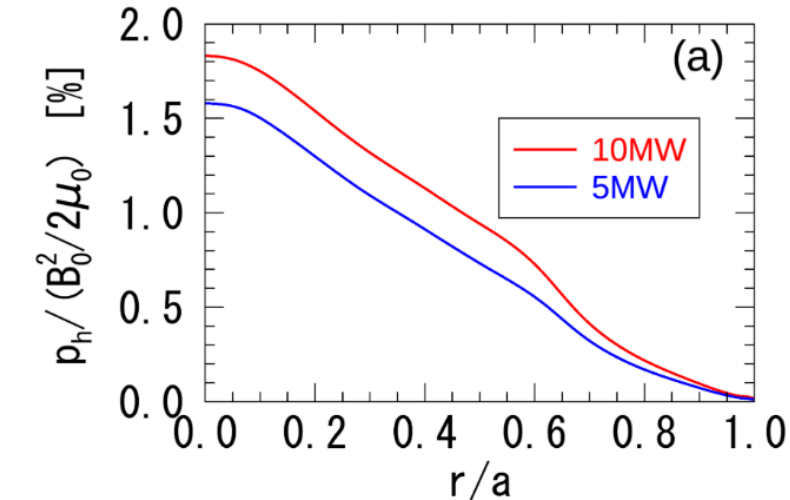
Collapse of stairway distribution and contribution of multiple modes to energy flux

collapse of stairway distribution

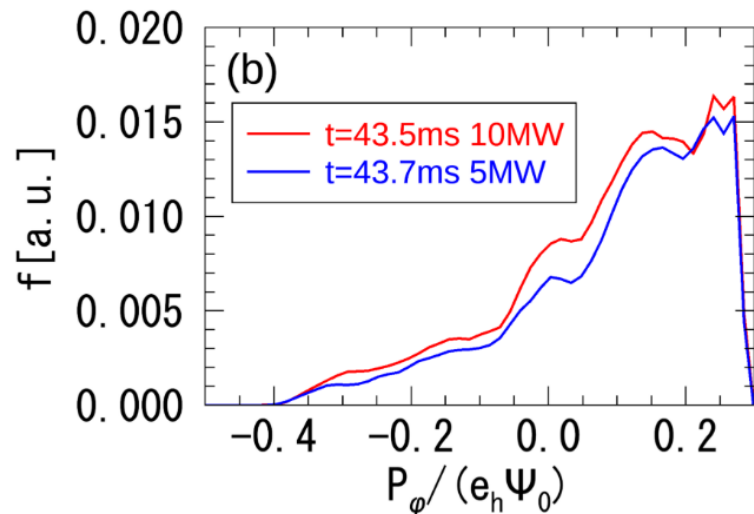


contribution of multiple modes to energy flux

Fast ion profile resiliency

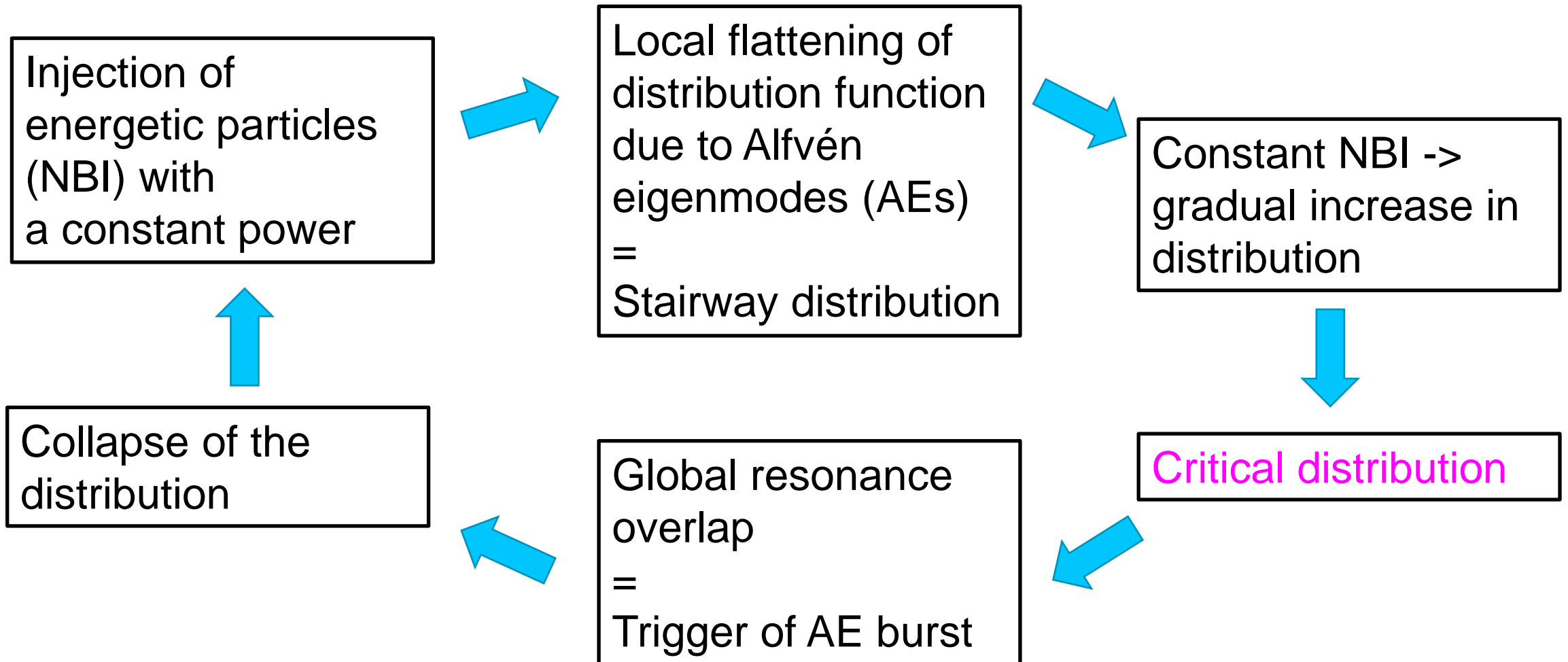


(a) Fast ion pressure rises only by 15% for doubled beam power = **profile resiliency**.



(b) Profile resiliency is found also for fast ion **distribution function** just before the bursts.

Summary



Summary of AE bursts (1)

- MEGA simulations of fast ion distribution formation process
 - for various beam deposition power (P_{NBI}) and slowing-down time (τ_s).
- With increasing volume-averaged classical fast ion pressure, the fast ion confinement degrades monotonically due to the transport by the Alfvén eigenmodes.
- For $P_{\text{NBI}}=10\text{MW}$ and $\tau_s=100\text{ms}$ (similar to the TFTR experiment)
 - AE bursts (=synchronized sudden growth of multiple AEs) take place
 - with a time interval $\sim 3\text{ms}$ and
 - the maximum amplitude $v_r/v_A=3 \times 10^{-3}$,
 - which are close to the TFTR experiment.

Summary of AE bursts (2)

- Before the sudden growth (=AE burst),
 - multiple AEs grow to low amplitude
 - low-amplitude AEs locally flatten the fast ion distribution
 - formation of a stairway distribution
- **The stairway distribution =“critical distribution”** where the further beam injection leads to
 - broadening of the locally flattened regions and their overlap
- The overlap of locally flattened regions (=resonance overlap) brings about
 - synchronized sudden growth of AEs and global transport of fast ions
 - **profile resiliency** = almost the same fast ion pressure profile and distribution function for 5MW and 10MW beam power

Summary

- Energetic particles (EPs) and Alfvén eigenmodes (AEs) in fusion plasmas
- Resonance condition, conserved quantity, and inverse Landau damping
- Phase space islands created by particle trapping and higher-order islands
- Nonlinear evolution of a bump-on-tail instability and frequency chirping
- Kinetic-MHD hybrid simulation
- Hybrid simulation for EP and MHD
 - Nonlinear MHD effects and zonal flow generation
 - Validation on DIII-D experiments (fast ion profile flattening and stiffness, electron temperature fluctuations)
 - AE burst and critical fast-ion distribution (profile resiliency)